

## Activity report of the Plasma Physics department

*V. Bagnoud<sup>1,2</sup>, A. Blažević<sup>1,2</sup>, B. Borm<sup>3</sup>, C. Brabetz<sup>1</sup>, C. Bruske<sup>1</sup>, U. Eisenbarth<sup>1</sup>, S. Götte<sup>1</sup>, D. Khaghani<sup>4</sup>, A. Kleinschmidt<sup>2</sup>, S. Kunzer<sup>1</sup>, T. Kühl<sup>1</sup>, P. Neumayer<sup>1</sup>, D. Reemts<sup>1</sup>, O. Rosmej<sup>1</sup>, V. Schanz<sup>5</sup>, D. Schumacher<sup>1</sup>, N. A. Tahir<sup>1</sup>, A. Tauschwitz<sup>1</sup>, L. Tymura<sup>1</sup>, D. Varentsov<sup>1</sup>, K. Weyrich<sup>1</sup>, S. Zaehner<sup>3</sup>, and B. Zielbauer<sup>1</sup>*

<sup>1</sup>GSI, Darmstadt, Germany; <sup>2</sup>HI Jena, Jena, Germany; <sup>3</sup>JWG University, Frankfurt Germany; <sup>4</sup>FS University, Jena, Germany; <sup>5</sup>TU Darmstadt, Darmstadt, Germany

The plasma physics department of GSI is responsible for the operation at three experimental facilities on the GSI campus, namely the Z6 experimental area at the UNILAC, the High Energy cave HHT at the SIS18 and the PHELIX laser facility. In addition, the department is strongly involved in the preparation of the FAIR experiments. Below is a summary of the highlights for 2017.

### Highlights from the Plasma Physics Program

In 2017, the study of the interaction of short laser pulses with matter was at the center of the research of the plasma physics department because of the direct applications of laser-driven diagnostics for FAIR.

In a series of experiments conducted with PHELIX, our group has shown that optical diagnostics can be employed to study the relativistic laser-plasma interaction at the femtosecond time-scale when the part of the pulse reflected [1] or transmitted [2] through thin targets is analysed. In particular, a method based on spectral interferometry has been used for the first time for the characterization of the relativistic laser-plasma interaction, showing evidence of interaction in the relativistic transparency regime.

In a second laser-plasma experiment at the Ti:sapphire laser JETI40 of the FSU Jena conducted by our group, ultra-high energy density plasma states with a keV bulk electron temperature, near-solid electron density and GBar pressure were diagnosed using x-ray spectroscopy tools. The generation of 150-nm thick plasma layers by irradiation of metallic foils at high laser temporal contrast and at the second harmonic laser frequency was explained by the collisional mechanism of the laser pulse absorption in a thin skin layer of plasma with a step-like electron density profile, followed by the electron heat transport. This scenario is opposite to the usually considered volumetric heating by supra-thermal electrons, which production was strongly suppressed [3].

In laser-plasma interaction, one of the central issues is the coupling efficiency of the laser energy into secondary particle or radiation. Using foam targets developing into plasmas at near critical plasma density is a way toward higher conversion efficiency of the laser energy into MeV electron beams. Such an experiment has been performed at the PHELIX, where preliminary results show dramatic increase of the supra-thermal electron energy far beyond ponderomotive one (16 MeV compared to 2 MeV) and strong increase of the total number of electrons with energies above 10 MeV (tens of nC). This was confirmed by measuring the gamma dose caused by bremsstrahlung. Both energetic electrons and gamma-rays are excellent candidates for radiographic applications in HED experiments [4].

Another route to enhance the yield of secondary radiation produced by intense laser pulses is the use of structured target surfaces. Thin metal foil targets covered with dense arrays of aligned high aspect ratio nano- and micro-wires have been produced at GSI in collaboration with the material science department and subjected to high-energy laser pulses from the PHELIX facility. Significant enhancement in both x-ray emission and proton acceleration has been demonstrated [5]. Irradiation of such delicate targets with the high-energy picosecond laser pulses has become feasible at the PHELIX facility due to the significant improvement of the laser pulse contrast over the past years.

Backlighting of mm-scale high-Z targets as foreseen in the FAIR plasma physics program will require hard x-ray radiation with photon energies above 100 keV, which can be produced by high-energy short-pulse laser systems. An experiment to extensively characterize the emission characteristics of such sources (conversion efficiency, angular and spectral distribution) over a wide range of laser parameters has been carried out at PHELIX [6], which provides important data towards the requirements for a future "Helmholtz beamline at FAIR". Also in this experiment, x-ray emission source sizes down to 5  $\mu\text{m}$  could be achieved using thin tungsten wires as generation target. Such small source sizes provide the necessary spatial coherence to realize x-ray phase contrast radiography. This was demonstrated in a subsequent campaign, where x-ray phase contrast imaging was used to diagnose laser-driven shock waves [7].

The LIGHT (Laser Ion Generation, Handling and Transport) experiments concerns the capture of laser accelerated ions by a conventional solenoid, their phase rotation in a rf-cavity, followed by their transport over longer distances before being refocused again for applications. Here, the focus of the investigations in 2017 was set to prepare the ion beam for an energy loss experiment in plasma [8]. In two experimental campaigns done at the Z6 target area, the proton beam at the end of the LIGHT beamline was further characterized, after the 6-m-long beam transport that includes a time-compression stage of the ion pulse and its spatial focusing with a pulse solenoid. At a proton energy of 8.1 MeV, the beam was focused down to 1.3 x 2 mm<sup>2</sup> with a peak current of 121 mA and a pulse duration of 500 ps, which is an improvement compared to the results obtained previously.

As the stopping power of protons is small, heavier ions would be preferable to employ the LIGHT beamline for heavy-ion energy-loss measurement experiments. Therefore, some time was dedicated to the generation and characterization of TNSA-driven carbon ions by heating tungsten foils evaporated with carbon to temperatures of

above 1000°C to remove the protons. The experiments showed that above an energy of 0.5 MeV/u C 4+ is dominating the spectrum and can be transported efficiently over longer distances by conventional accelerator components. The results are very promising when regarding these short (<500 ps) pulses as probe for energy loss experiments of heavy ions in laser generated plasma.

### Operation and Improvements of PHELIX

PHELIX has continuously delivered beam time to the international user community for the last nine years. In 2017, its operation profile was, as in previous years, distributed between maintenance and upgrade phases and beam-time operation (52%) as shown in Figure 1. The operation plan has been impacted in summer when a mandatory fire-safety-relevant building rehabilitation had to be made. During this time however, a long-standing survey and upgrade of the control system has taken place such that the shut-down time could be as efficiently used as possible.

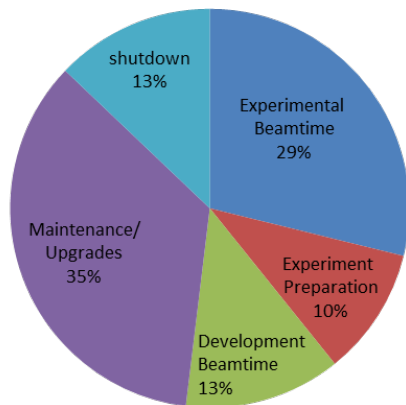


Figure 1: Operation profile of PHELIX in 2017.

In total 10 experiments have been conducted at PHELIX, which can be separated in 150 shifts dedicated to external users and 46 shifts used for the internal program of the LIGHT experiment at the Z6 experimental place [8]. The topics of the experiments vary from the first demonstration of x-ray phase-contrast imaging with the small spatially limited keV secondary sources generated by our group to the test of new liquid-crystal targets. Again, laser-driven acceleration has been at the topic of many of the experiments. PHELIX has been during this time, as in the past, very reliable with less than 5% of the shots as failed shots registered, thereof only 1.7% of the shots failed because of hardware-related issues.

Improvements to the facility have been performed on many of its sub-systems in 2017. A major on-going project is the upgrade of the PHELIX pre-amplifier to an architecture allowing for a 10-fold increase of its repetition rate. In 2017, the upgrade of the amplifier was completed during one of the maintenance phase early in the year, such that all the short-comings found during the commissioning done in 2016 could be fixed. Together with work done on the beam quality control, PHELIX could deliver in 2017 the nominal beam size of 28 cm as standard aperture which corresponds to an energy of 200 J at the end of the amplifier chain for short pulse experi-

ments and 300 J for nanosecond pulses used at the Z6 experimental area before frequency conversion. Note that this energy is limited right now for the short-pulse option by the diffraction gratings of the compressor that show some sign of ageing and are therefore run at a maximum laser fluence of 0.85 J/cm<sup>2</sup>.

Another major on-going project for the facility is the development of a VISAR system at the Z6 experimental place that turns the existing preliminary device developed in collaboration with the Technical University of Darmstadt to a reliable and versatile system that can be offered as a standard diagnostics tool to the users community, as recommended by the PHELIX committee. In 2017, the system has undergone the necessary upgrade that includes work on the laser source (better temporal coherence) and its interferometer (improved setup stability). Already in 2018, users will employ this diagnostic tool as their main diagnostic.

Developments on optical temporal diagnostics went on. Here the detection system of the short-pulse 3 $\omega$ -cross-correlator named EICHEL[9] was improved further to make it more insensitive to pulse-to-pulse energy fluctuations. First tests were conducted at the Polaris laser at HI Jena. In addition, EICHEL was used to characterize the temporal contrast of PHELIX when its linear regenerative amplifier is by-passed, showing an important reduction of the number of pre-pulses in the -1 to -2 ns time window before the peak of the pulse. An upgrade of PHELIX to include this by-pass should happen in the next months to exploit this new finding.

### PHELIX Committee 12, 2017

In spring 2017, a call for proposals synchronized to the general call for proposals of the GSI accelerator was made. This call is embedded in the strategy of GSI to offer beam time to the FAIR collaborations at GSI's facilities during the build-up phase of the new accelerator: the so-called phase 0 program. The PHELIX committee met during the summer and granted 11 laser-only proposals with beam time plus one combined laser-ion experiment. At the HHT and Z6 caves, 4 additional experiments have been granted access to the ion facility. In total, this amounts to a 42% success rate for applicants. The high demand on GSI's plasma physics facilities illustrates the vitality of the field and their attractiveness

### Progress on the FAIR Ion Facility for Plasma Physics

During the workshop on high-energy-density physics in Hirschegg, the community has decided to found a new collaboration called HED@FAIR, which aims at overtaking the responsibilities of the two previous collaborations involved in the FAIR project. One of the consequences of this move has been to raise interest in the planned experiments from further groups, e.g. the Chinese community that increased its contacts with our group. Negotiations to give Chinese groups a leading role in the plasma physics program at FAIR took place along the year, for instance during the EMMI workshop at GSI and the 1<sup>st</sup> Workshop for International Collaboration on High Energy Density

Science at FAIR and HIAF. The latter was held with about 70 participants from China and Germany in Xi'An, China. Participants from the Institute of Physics (Beijing), Peking University (Beijing), Laser Fusion Research Center (Mianyang), Xi'an Jiaotong University (Xi'an) and Shanghai Jiaotong University (Shanghai) showed interest to be part of the collaborative effort. The workshop resulted finally in a memorandum of understanding between the University of Xi'An and GSI.

The preparation for the FAIR phase 0 program, that will be conducted from 2018 on at the existing plasma physics experimental areas at GSI is well ongoing. Four experimental proposals dealing with the proton microscopy set up PRIOR have been submitted and all of them granted with beam time. To gather experience on proton microscopy technology and get a head-start with experiments, the proton microscope will be set up at HHT using part of the GSI contribution to FAIR. The in-kind contract with FAIR for financing the magnets and power supplies has been signed and the detailed specification written, so that the magnets can be ordered in 2018. Later on, the PRIOR system will be transferred to the FAIR building for HED@FAIR experiments, called APPA cave, where the plasma physics experiments at FAIR will be performed.

A second experiment platform to be made available at GSI for the phase-0 period is a target chamber for the HIHEX (Heavy Ion Heating and Expansion) scheme. This target chamber should be complemented with an arm of the PHELIX laser sent to HHT to volumetrically diagnose the samples generated by the ion beam already during the upcoming years. For this purpose, preliminary conceptual work has been performed and discussions on the various possible experiments took place during the EMMI workshop on plasma physics at FAIR that took place in the summer of 2017 at GSI. In particular, this target station could exploit the  $10^{11}$  Ni ions per bunch at an energy of 200-400 MeV/u available from the SIS-18 for the HIHEX scheme. With the existing HHT-focusing system, one can reach a Ni-beam specific energy deposition in to Al - Pb from 4 up to 16 kJ/g (cooled ion beam), which should be enough to start the scientific program of the plasma physics community at FAIR.

The planning of the APPA cave is progressing well and should be finalized in 2018. Concerning the experimental equipment in the APPA cave the last Technical Design Report relevant for the day-1 experiments is approved and the technical board of HED@FAIR is now concentrating more and more to the definition of the detailed specifications and ordering of the components, while the final focussing system, consisting of 4 super conduction large aperture quadrupoles, has been contracted with the Institute of High Energy Physics in Protvinov, Russia, and is now in the final design phase.

Concerning the science program for plasma physics at FAIR, hydrodynamical simulations using the code BIG2 have shown that the ion parameters expected at FAIR in the APPA cave, namely uranium ion intensities from  $10^{11}$  to  $5 \times 10^{11}$  ions/pulses, are very appropriate to realize low-temperature compression of iron using the LAPLAS (LABoratory PLANetry Science) scheme to conditions relevant to earth and super-earth core conditions [10]. In this proposed experiment, an annular ion beam quickly heats a

tungsten temper that compresses a cold iron inner core. The maximum pressure accessible using FAIR by varying the number of ions in the pulse is in the range of 2 to 7 Mbar. In addition, the temperature of the iron pay load is independently tuned by changing the amount of ions leaking on axis. In such conditions, the temperature achievable during compression can be as low as 0.1 eV (no ions on axis) and continuously increased to 2 eV when the ion density on axis reaches 20% of the ring density. All-in-all, these parameters cover the range of pressures and temperatures necessary to study earth core and super-earth core conditions in the laboratory. This type of experiments could extend the current data obtained by diamond anvil cells on iron to the WDM region relevant to planetary science.

## References

- [1] J. Hornung et al., this report
- [2] V. Bagnoud et al., PRL **118**, 255003 (2017)
- [3] O. Rosmej et al., submitted to PoP
- [4] S. Zaether et al., this report
- [5] D. Khaghani et al., Scientific Reports **7**, 11366 (2017)
- [6] B. Borm et al., this report
- [7] L. Antonelli et al., this report; L. Antonelli et al., submitted to PRL
- [8] D. Jahn et al., this report and J. Ding et al, R. Leonhard et al, this report
- [9] V. A. Schanz et al., Opt. Express **25**, 8 (2017)
- [10] N. A. Tahir et al., this report; N. A. Tahir et al., The Astrophysical Journal Supplement Series **232**, 1 (2017)

## X-ray Phase-Contrast Imaging for Laser-induced shock-wave

L. Antonelli<sup>1,2</sup>, F. Barbato<sup>3</sup>, J. Trela<sup>4</sup>, D. Mancelli<sup>4</sup>, G. Zeraoui<sup>5</sup>, A. Atzeni<sup>1</sup>, A. Schiavi<sup>1</sup>, G. Boutoux<sup>4</sup>, L. Volpe<sup>5</sup>, P. Bradford<sup>2</sup>, N. Woolsey<sup>2</sup>, V. Bagnoud<sup>6</sup>, C. Brabetz<sup>6</sup>, P. Neumayer<sup>6</sup>, B. Zielbauer<sup>6</sup>, B. Borm<sup>6</sup> and D. Batani<sup>4</sup>

<sup>1</sup>University of Rome „La Sapienza“, Rome, Italy; <sup>2</sup>University of York, York, UK; <sup>3</sup>EMPA, Zurich, Switzerland; <sup>4</sup>University of Bordeaux, Talence, France; <sup>5</sup>CLPU, Salamanca, Spain; <sup>6</sup>GSI, Darmstadt, Germany; <sup>4</sup>Goethe University, Frankfurt-M, Germany

X-ray Phase-Contrast Imaging (XPCI) is a technique where the phase-shift induced by a density gradient is used to enhance a diffraction pattern in an X-ray image. This well-known technique is normally applied in biology and medicine because it is ideal to make visible any interface where a change of density is present. In high energy density science experiments the sensitivity to density gradients is ideal to probe hydrodynamic instabilities as well as shock front degradation [1,2] which could be caused by the presence of hot electrons which could cause a non-uniform target temperature.

In our experiment at GSI we used the laser PHELIX to generate X-ray pulses with a limited source size. The aim of our experiment was to demonstrate the feasibility of single-shot XPCI using short-pulse (picosecond) laser-driven X-ray bremsstrahlung emission sources. The necessary small source size if achieved using tungsten wires with a diameter of 5  $\mu\text{m}$  as targets to produce the x-ray source [3], which were developed in a previous beamtime at the PHELIX laser. We used this X-ray flash to obtain XPCI of static objects as well as to probe a laser-induced shock-wave propagating in a polystyrene cylinder irradiated with long-pulse (nanosecond) beam.

Figure 1 shows experimental XPCI images obtained in the experiment. Nylon wires with a range of diameters were used as static test objects. The presence of phase contrast enhancement in these images is clearly visible where interface surface are located. Because we are using an incoherent broadband spectrum light source the phase contrast is given by the so called lateral coherence defined as:

$$l_t \approx \frac{R_0 \lambda}{s}$$

where  $R_0$  is the source-target distance,  $\lambda$  the incidence X-ray wavelength and  $s$  the source size. In our case an average value of the lateral coherence was 10  $\mu\text{m}$  which guarantees the possibility to probe steep density gradient in our target. Using the double-pulse option of the PHELIX

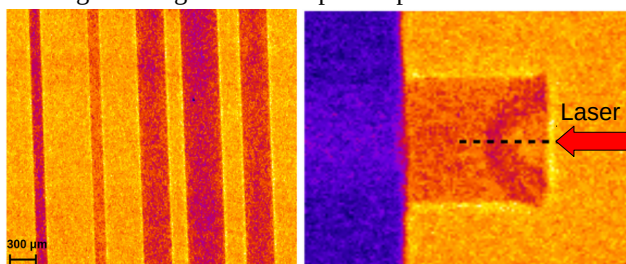


Figure 1: XPCI images taken with the laser-generated x-ray source of (left) Nylon wires and (right) a laser-driven shock propagating into a cylindrical target.

laser we have also demonstrated XPCI in a pump-probe scheme, using one of the laser pulses to drive a strong shock into a sample (Fig. 1, right). The radiographic image shows the shock-front at a time of 6 ns after the end of the drive laser pulse. The presence of phase contrast is evident at the target-vacuum interface, as well as at the shock-front. In addition, we observe phase contrast in the central part of the shock-wave. This is attributed to the rarefaction wave propagating inside the shock lowering the pressure.

This first proof-of-principle experiment shows how this technique can provide a deeper insight in the shock physics underline details which would not be present with a conventional X-ray absorption radiography. Moreover, this experiment validate the feasibility of the technique on intermediate-scale laser facilities, but can also be applied on larger scale facility like OMEGA or NIF.

What is required is the capability to control the source dimension and this can be successfully achieved using mass limited target or pin-hole.

XPCI due to its intrinsically sensibility to density gradient is the ideal diagnostic to probe hydrodynamic instability as well as shock front degradation which could be caused by the presence of hot electron which could cause a non-uniform target temperature.

## References

- [1] A. Schropp et al., SCI REP-UK 5, 11089 (2015).
- [2] J. Workman et al., Rev. Sci. Instrum. 81, 10E520 (2010).
- [3] B. Borm *et al.*, GSI Scientific Report 2017

**Experiment beamline:** PHELIX

**Experiment collaboration:** none

**Experiment proposal:** P133

**Accelerator infrastructure:** none

**PSP codes:** none

**Grants:** This work benefited from the support of COST Action MP1208 'Developing the physics and the Scientific Community for Inertial Fusion' and by the EUROfusion project "Preparation and Realization of European Shock Ignition Experiments". The research leading to these results has received funding from LASERLAB-EUROPE (grant agreement no. 654148, European Union's Horizon 2020 research and innovation programme).

## Ultra-high magnetic field generation in curved targets: A novel approach to laboratory astrophysics and laser-based applications

*P. Korneev<sup>1,2</sup>, J.J. Santos<sup>3</sup>, M. Ehret<sup>3,5</sup>, Y. Abe<sup>6</sup>, F. Law<sup>6</sup>, Y. Kochetkov<sup>1</sup>, V. Stepanishchev<sup>1</sup>, S. Fujioka<sup>6</sup>, E. d'Humieres<sup>3</sup>, V. Bagnoud<sup>4</sup>, B. Zielbauer<sup>4</sup>, G. Schaumann<sup>5</sup>, M. Roth<sup>5</sup>, V. Tikhonchuk<sup>3</sup>*

<sup>1</sup>NRNU MEPhI, Russian Federation; <sup>2</sup>Lebedev Institute, Russian Federation; <sup>3</sup>CELIA, Université de Bordeaux, France; <sup>4</sup>GSI, Darmstadt, Germany; <sup>5</sup>IKP TU-Darmstadt, Germany, <sup>6</sup>ILE, Osaka University, Japan;

Optical-based magnetic field generation is a convenient tool for applications, including particle guiding, laboratory based astrophysical-related studies and studies of matter behaviour in magnetic fields. The goal of this experimental campaign was a detailed study of a novel recently proposed scheme of such generation, in which a relativistic laser pulse interacts with a cylindrically shaped target [1], performing multiple reflections along the internal target surface (see Fig.1). In these conditions, the laser pulse generates relativistic electrons, propagating along the surface, and, consequently, return currents in the target bulk, which are responsible for the magnetic field generation.

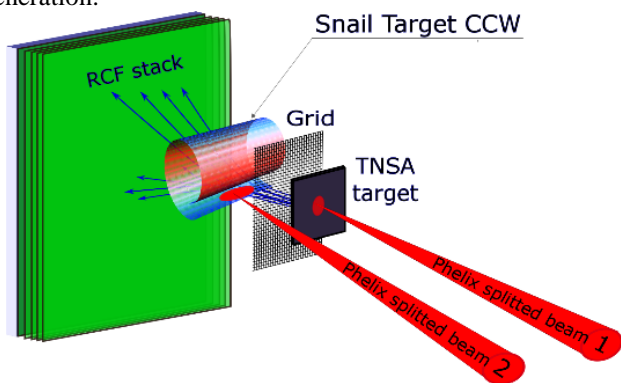


Figure 1: Principal experimental setup for generation of magnetic fields in snail-shaped target. Proton deflectometry diagnostic is shown; optical (polarimetry and interferometry) and  $K\alpha$  diagnostics are not shown.

In the experimental campaign, the PHELIX laser beam was splitted in two, one used as a target driver (CP1), and another (CP2) as a TNSA proton generator when interacting with a gold foil with 4  $\mu\text{m}$  thickness. Besides the main target and the foil, a fine mesh was aligned on the way of TNSA protons for better resolution of proton deflection in

the diagnosed fields. Optical diagnostics (polarimetry and interferometry) was also performed.

About twenty successful shots gave the information about the generated field structure, its time-dependence, and strength. A sample RCF image with a preliminary analysis is presented in Fig. 2. The observed shape of detected diagnostic protons is in a good agreement with the test-particle modelling of deflected TNSA protons, assuming a  $\sim 500\text{T}$  magnetic field in the target generated by solenoidal-like currents. Preliminary analysis of the experimental data for different time delays between CP1 and CP2 shows that the magnetostatic structure is stable for  $\sim 80$  ps, which is of the hydrodynamic scale of the target expansion.

The obtained experimental data are being processed yet, but already we can state several important results: the snail-shaped targets are efficient quasi-static magnetic field generators with the time-of-life of the magnetized structures being of the hydrodynamic time scale. The experimental study opens new perspectives for optical-based magnetic field generation and applications.

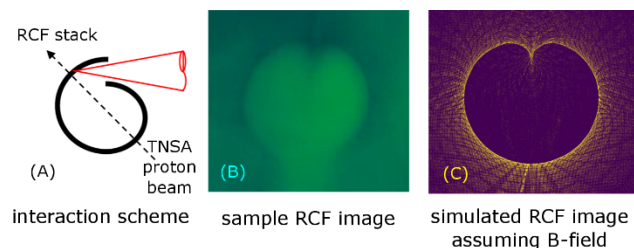


Figure 2: (A) a sketch of the principal experimental setup, (B) an example RCF image (from preliminary experimental results), (C) test-particle modelling of proton deflectometry image, assuming a solenoidal generated magnetic field of  $\sim 500\text{T}$  in the target.

### References

- [1] Ph. Korneev et.al., Phys.Rev. E 91, 043107 (2015)

**Experiment beamline:** PHELIX  
**Experiment collaboration:** none  
**Experiment proposal:** P136  
**Accelerator infrastructure:** none  
**PSP codes:** none

**Grants:** 2015-2019 grant of the Institut Universitaire de France obtained by CELIA, Russian Foundation for Basic Research (# 16-52-50019 ЯФ), Excellence program NRNU MEPhI (contract No. 02.a03.21.0005, 27.08.2013), Program of Increase in the Competitiveness of the National Research Nuclear University MEPhI. The EUROfusion Consortium and the Euratom research and training programmes 2014-2018 under grant agreement No 633053 and 2017-2018 under grant agreement No CfP-AWP17-IFE-CEA-02. The views and opinions expressed herein do not necessarily reflect those of the European Commission.

**Strategic university co-operation with:** Darmstadt

## Fourier transform spectral interferometry as plasma diagnostics

V. Bagnoud<sup>1,2</sup>, J. Hornung<sup>1,2</sup>, T. Schlegel<sup>1,2</sup>, B. Zielbauer<sup>1</sup>, C. Brabetz<sup>1</sup>, M. Roth<sup>3,4</sup>, P. Hitz<sup>5</sup>,  
M. Haug<sup>5</sup>, J. Schreiber<sup>5</sup>, and F. Wagner<sup>1,2</sup>

<sup>1</sup>GSI, Darmstadt, Germany; <sup>2</sup>HI Jena, Jena, Germany; <sup>3</sup>Technische Universität Darmstadt, Darmstadt, Germany;  
<sup>4</sup>FAIR, Darmstadt, Germany; <sup>5</sup>Ludwig-Maximilians-Universität, Garching, Germany

The interaction of short laser pulses of the highest intensities with thin sub-micrometer foils has received lots of attention in the last years because of its potential applications to laser-driven particle acceleration and the generation of hard x-rays that could be prime diagnostics for the FAIR facility for instance. In the last years, these studies were made possible by the ever-increasing temporal qualities of short laser pulses delivered by the most modern laser systems. While thin sub-micrometer foils used to be fully blown off many 10's of picosecond before the interaction with the main part of the pulse had begun, the latest generation of lasers with ultra-high temporal contrast like PHELIX enables such an interaction to happen. Yet, the exact status of the foil at the time of the interaction remains unclear and should be studied in details. Here, we have shown that the use of a second pulse that interrogates the plasma after the interaction with the first one is possible using standard spectroscopic methods [1]. It is possible to analyse the signal  $S(\omega)$  by Fourier transformation with a technique known as Fourier-transform spectral interferometry (FTSI) that was proposed and demonstrated more than 20 years ago [2]. To understand the underlying mathematics, let us define the electric field of laser pulse as:

$$E(t) = A(t)e^{i\omega_0 t} \quad (1)$$

where  $A$  is the complex amplitude of the field and  $\omega_0$  the carrier angular frequency of the pulse. After propagation through the plasma, the field is modulated by a complex function  $T(t)$  whose modulus describes the time-dependent transmission through the foil and its argument temporal phase effects, like relativistic self-phase modulation or electron blow-out. When two pulses delayed by  $\tau$ , of fields  $E_1$  and  $E_2$ , cross a plasma and their amplitude is modulated by  $T_1$  and  $T_2$ , the total field after the plasma can be described as:

$$E(t) = A_1(t)T_1(t)e^{i\omega_0 t} + A_2(t)T_2(t)e^{i\omega_0(t-\tau)} \quad (2)$$

A spectrometer that analyses the resulting pulses shows a signal  $S$  exhibiting an interference that is given by:

$$\begin{aligned} S(\omega) &= |E(\omega)|^2 \quad (3) \\ &= |FT(A_1(t)T_1(t)e^{i\omega_0 t}) + FT(A_2(t)T_2(t)e^{i\omega_0 t})e^{-i\omega_0 \tau}|^2 \\ &= |E_1(\omega)|^2 + |E_2(\omega)|^2 + 2\cos(\omega\tau + \Delta\varphi) |E_1(\omega)E_2(\omega)| \end{aligned}$$

where  $E_{1,2}(\omega)$  is the complex spectral amplitude of the pulses after transmission through the plasma and  $\Delta\varphi$  the spectral phase difference between both pulses with:

$$E_{1,2}(\omega) = FT(A_{1,2}(t)T_{1,2}(t)e^{i\omega_0 t}) \quad (4)$$

In eq. 3, the information about the amplitude  $|E(\omega)|$  and spectral phase difference  $\Delta\varphi$  is somehow entangled. However, when  $\tau$  is chosen such that the fringes are still resolved by the spectrometer but fine enough so that the interference resolves the spectrum modulations, an analysis in the Fourier domains yields three peaks that can be numerically isolated and inverse Fourier-transformed to yield  $|E_1(\omega)|$ ,  $|E_2(\omega)|$  and  $\Delta\varphi$  at once.

The experimental demonstration was done during the beamtime P126 granted at the PHELIX facility with the setup shown in fig. 1. More details can be found in [1].

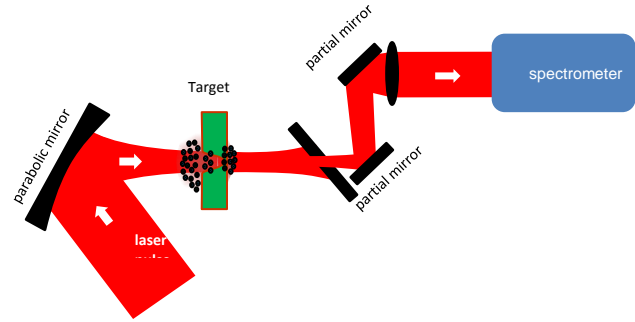


Figure 1: Experimental setup of experiment P126 that enables measuring the spectral interference for FTSI.

In our implementation the second pulse has an intensity ratio of a few percent to the main pulse and it was generated in the front end of PHELIX. Our analysis has shown that one can easily retrieve the difference in transit delay through the plasma, showing that for the thinnest targets, the plasma is relativistically transparent [1]. In addition, coupled to a FROG [3], the full temporal structure of the pulses  $E_1(t)$  and  $E_2(t)$  after the interaction can be reconstructed.

Further experiments could be planned in the near future to study the plasma dynamics by varying the delay  $\tau$  for instance.

## References

- [1] V. Bagnoud, J. Hornung, T. Schlegel, et al. "Studying the Dynamics of Relativistic Laser-Plasma Interaction on Thin Foils by Means of Fourier-Transform Spectral Interferometry" *Phys. Rev. Lett.* **118** 255003 (2017)
- [2] L. Lepetit, G. Chériaux, and M. Joffre. "Linear techniques of phase measurement by femtosecond spectral interferometry for applications in spectroscopy" *JOSA B* **12**, 2467 (1995)
- [3] F. Wagner, J. Hornung, C. Schmidt, et al. "Backreflection diagnostics for ultra-intense laser plasma experiments based on frequency resolved optical gating" *Review of Scientific Instruments* **88** (2017) 023503

**Experiment beamline:** PHELIX  
**Experiment collaboration:** APPA-HED@FAIR  
**Experiment proposal:** P126  
**Accelerator infrastructure:** none  
**PSP codes:** none  
**Grants:** Transregio 18  
**Strategic university co-operation with:** Darmstadt

## Relativistic interaction of mid-infrared laser pulses with nanowire targets: towards a novel laser-plasma interaction regime

Z. Samsonova<sup>1,2</sup>, S. Höfer<sup>1</sup>, V. Kaymak<sup>3</sup>, S. Ališauskas<sup>4</sup>, V. Shumakova<sup>4</sup>, A. Pugžlys<sup>4</sup>, A. Baltuška<sup>4</sup>, T. Siefke<sup>1</sup>, S. Kroker<sup>5</sup>, O. Rosmej<sup>6</sup>, A. Pukhov<sup>3</sup>, I. Uschmann<sup>1</sup>, C. Spielmann<sup>1,2</sup>, and D. Kartashov<sup>1</sup>

<sup>1</sup>IOQ & IAP, Friedrich-Schiller-University Jena, Germany; <sup>2</sup>Helmholtz Institute Jena, Germany; <sup>3</sup>Heinrich-Heine-University Düsseldorf, Germany; <sup>4</sup>Vienna University of Technology, Austria; <sup>5</sup>LENA, Technical University Braunschweig, PTB, Germany; <sup>6</sup>GSI, Darmstadt, Germany.

In this report we present the results of the investigation of the relativistic mid-infrared laser pulses with silicon targets. The novelty of this regime lies in the scaling of the interaction parameters such as plasma critical density and normalized vector potential with the wavelength [1]. It also means that for mid-IR pulses the ionization happens in the tunnel regime, which in contrast to one/multiphoton ionization allows sharp plasma density gradients. These new features strongly influence the parameters of created plasmas, thus, generated X-ray emission. The use of nanostructured targets may additionally enhance the effect due to the high laser energy absorption shown in earlier works [2-4]. In order to investigate the possibility to generate extreme plasma states we compare the line emission spectra and bremsstrahlung emission generated from different targets, and apply PIC simulations together with kinetic FLYCHK code to match our experimental findings and the theoretical predictions.

### Experiment & Results

The p-polarized idler beam of OPCPA laser system (TU Vienna) with energy of 25 mJ is focused under 45° onto the samples resulting in the peak intensity of nearly  $10^{17}$  W/cm<sup>2</sup> with a pulse duration of 90 fs. The generated X-ray emission is then detected with the crystal spectrometer and the Timepix detector in a single shot. It is shown, that the intensity of the K-shell emission from neutral atoms as well as the hard X-ray bremsstrahlung are comparable for polished and nanowire (NW) targets. However, the efficiency of the line emission from highly charged ion states differs dramatically. In case of the polished sample there is essentially no emission from the transitions in He- and H-like Si observed (Fig. 1). This means that the electron density and bulk electron temperature are higher for the NW target.

### Simulations & Discussions

To estimate the achieved plasma parameters we attempted to fit the experimental X-ray spectra with the synthesized ones using the temporal evolution of the parameters predicted by the PIC code. In case of NWs, the bulk electron temperature reaches its maximum value in the keV range by the end of the laser pulse, while the electron density exceeds solid density in the whole volume of nanowires. Corresponding X-ray line emission spectrum matches well to the hot part of the experimental spectra (Si<sup>12+</sup>-Si<sup>13+</sup>). The PIC simulations for the polished target are more troublesome requiring an inclusion of the spatial distribution of the laser intensity and higher resolution. However, assuming similar time scale for plasma

cooling and its recombination and introducing a two-parameter search over the maximum bulk electron temperature and density we achieve a good agreement between the simulations and the experimental results for the maximum electron density about  $10^{23}$  cm<sup>-3</sup> and the bulk temperature of several hundred eV. The severe difference may arise from the larger penetration depth and higher absorption of the laser pulse within the NWs. Remarkably, the predicted electron density exceeds the critical density calculated for the used mid-infrared pump by 3 orders of magnitude.

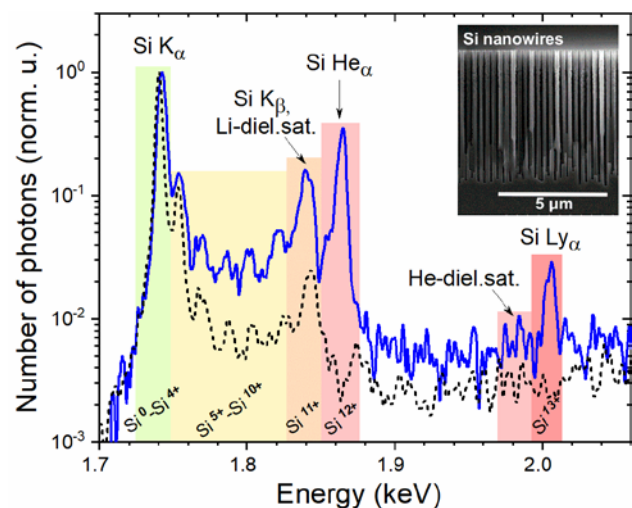


Figure 1: K-shell emission spectra for the polished (black dashed) and the NW (blue solid) Si targets. Inset: SEM image of the NW array.

Our studies demonstrate that relativistically intense ultrashort laser pulses in mid-IR spectral range are capable to generate solid density and keV-temperature plasmas and using NW targets may significantly increase the efficiency of the impact ionization and plasma heating.

### References

- [1] J. Weisshaupt et. al., Nat. Phot. 8, 927-930 (2014).
- [2] T. Nishikawa et. al., Appl. Phys. B 78, 885 (2004).
- [3] S. Mondal et. al., Phys. Rev. B 83, 035408 (2011).
- [4] M. A. Purvis et. al., Nat. Phot. 7, 796-800 (2013).

**Experiment beamline:** none

**Experiment collaboration:** none

**Experiment proposal:** none

**Accelerator infrastructure:** none

**Strategic university co-operation with:** Vienna, Austria

\*This report is also submitted to the HI Jena Annual Reports 2017



## X-ray generation by laser hole boring and channelling in dense plasma

R. Wilson<sup>1</sup>, B. Gonzalez-Izquierdo<sup>1</sup>, M.J. Duff<sup>1</sup>, C. Armstrong<sup>1,2</sup>, R.J. Gray<sup>1</sup>, M. King<sup>1</sup>,  
C. Brabetz<sup>3</sup>, B. Zielbauer<sup>3</sup>, V. Bagnoud<sup>3</sup>, D. Neely<sup>2,1</sup> and P. McKenna<sup>1</sup>

<sup>1</sup>SUPA, Department of Physics, University of Strathclyde, Glasgow, G4 0NG, United Kingdom; <sup>2</sup>Central Laser Facility, STFC Rutherford Appleton Laboratory, Didcot, Oxfordshire, OX11 0QX, United Kingdom; <sup>3</sup>PHELIX Department, GSI Helmholtz Center for Heavy Ion Research, Planckstrasse 1, D-64291, Germany

### Introduction

We report on an experiment which aimed to investigate the sensitivity of X-ray radiation generation to the degree of laser channelling occurring in overdense plasma. Channelling is driven by the processes of relativistic self-induced transparency (RSIT) [1] and radiation pressure hole boring (HB) [2] and enables the laser to interact with the target plasma volumetrically. X-rays are produced by electron acceleration in the fields generated, or via Bremsstrahlung due to interaction with the fields of the target atoms, and provide a useful diagnostic due to their penetration through the dense target, enabling the channelling dynamics to be probed. Investigation of laser hole-boring and channelling physics in dense plasma at the upper limits of intensities achievable today ( $\sim 10^{21}$  Wcm<sup>-2</sup>) benchmarks models used to design future experiments at multi-petawatt lasers, for which radiation pressure driven effects will dominate the physics.

### Experiment

The experiment was conducted using the PHELIX laser. This system is one of few capable of routinely achieving peak intensities up to mid- $10^{20}$  Wcm<sup>-2</sup>, which are required to probe radiation pressure-driven phenomena. This system can deliver 200 J pulses ( $\sim 155$  J on-target) with a duration of 700 fs (FWHM). The high temporal intensity contrast delivered ( $\sim 10^{11}$  [3]) is also critical for experimentation using ultra-thin (nanometre scale) and low density foam type targets, to prevent significant target expansion prior to the arrival of the peak laser energy.

To investigate X-ray generation, a complementary suite of diagnostics were implemented to characterise both the spectral and spatial distributions, and source size. These included a crystal spectrometer operating in the range 17-200 keV, a scintillator-based array diagnostic, which provides low resolution spatial and spectral measurements extending to the hard X-ray range, and a high resolution ( $\mu\text{m}$ ) penumbral imaging system to quantify the X-ray source size.

Additionally, a curved stacked detector [4], consisting of image plate and steel filters, was placed around the interaction region. This provides a high resolution angular and low resolution energy measurement of the distribution of electrons which 'escape' the target foil. Furthermore, the degree of laser light both reflected from and transmitted through the target was measured. This not only enables the plasma absorption dynamics to be probed, but additionally enables the conditions for the onset of transparency to be determined. Pictures of the experimental set-up in the PHELIX target chamber are shown in Fig. 1.

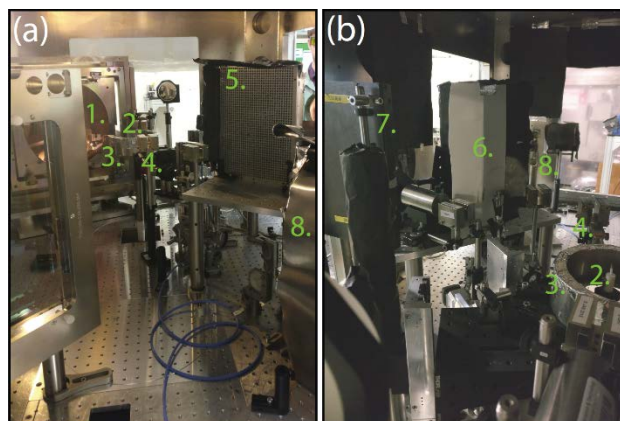


Figure 1: (a) and (b) Photographs of the experimental set-up, where the labels identify the main components as follows; 1. off-axis parabola, 2. target, 3. curved stacked detector, 4. penumbral imager, 5. scintillator array, 6. laser transmission screen, 7. electron spectrometer and 8. X-ray crystal spectrometer.

The targets selected for exploring X-ray generation were relatively thin (40-1000 nm) foils (Al, Au and CH) and low density plastic based foam targets (25-500 mg/cm<sup>3</sup>), in order to investigate the transition from surface-dominated physics to volumetric interaction induced by HB and RSIT.

Analysis of the data measured on the experiment is currently underway, and results will be reported in future publications.

### References

- [1] V.A. Vshivkov et al. Phys. Plasmas 5, 2727 (1998).
- [2] S.C. Wilks et al Phys. Rev. Lett. 69, 1383 (1992).
- [3] F. Wagner et al. Appl. Phys. B 116, 429 (2014).
- [4] R.J. Gray et al. Appl. Phys. Lett. 99, 171502 (2011).

**Experiment beamline:** none

**Experiment collaboration:** other: PHELIX

**Experiment proposal:** P124

**Accelerator infrastructure:** other: PHELIX

**PSP codes:** none

**Grants:** EP/J003832/1, EP/L001357/1 and EP/K022415/1

**Strategic university co-operation with:** none

## A pump-probe technique for laser-driven proton beam heating to warm, dense states with the PHELIX laser

C. McGuffey<sup>1</sup>, C. Brabetz<sup>2</sup>, M. Dozieres<sup>1</sup>, J. Kim<sup>1</sup>, M. Bailly-Grandvaux<sup>1</sup>, P. Forestier-Colleoni<sup>1</sup>, F. N. Beg<sup>1</sup>, M. Roth<sup>3</sup>, V. Bagnoud<sup>2</sup>

<sup>1</sup>University of California San Diego, La Jolla, CA, 92071, U.S.A.; <sup>2</sup>GSI Helmholtzzentrum für Schwerionenforschung, Plasma Physik/PHELIX, Darmstadt, Germany; <sup>3</sup>Institut für Kernphysik, Technische Universität Darmstadt, Darmstadt, Germany

### Conceptual technique for warm dense matter creation and characterization

Warm Dense Matter (WDM) is a scientifically interesting thermodynamic state falling in between the descriptions of condensed matter and plasma. WDM samples can be produced, for example, by rapid isochoric heating by an intense proton beam driven by a short pulse laser. We used the double short pulse beam capability of the PHELIX facility ( $\leq 100$  J,  $\geq 0.5$  picosecond) to begin developing a pump/probe method.

The main split of the laser (35 J,  $1 \times 10^{19}$  W/cm<sup>2</sup>) was delivered to curved 10  $\mu$ m thick diamond-like carbon foils to generate protons through the target normal sheath acceleration mechanism [1]. The protons heated a tamped sheet of Cu edge-on. The second split of the laser (20 J,  $6 \times 10^{18}$  W/cm<sup>2</sup>) was delivered to a backlighter target using an independent parabolic mirror and delay stage. This produced a broadband x-ray strobe, face-on to the Cu foil, allowing x-ray absorption spectroscopy through the thin dimension (100 nm). The conceptual configuration is shown in Figure 1.

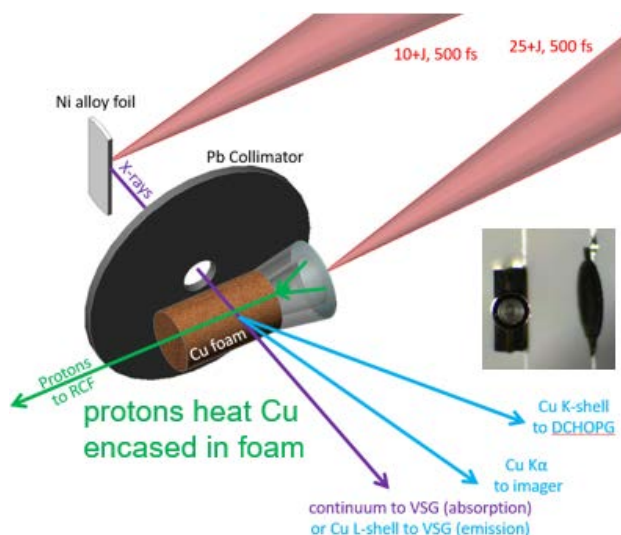


Figure 1: Conceptual setup with a Cu foam target variation. The baseline target used an upright solid Cu foil with plastic tamp walls and built-in aperture in place of the Cu foam (inset shows a real target as seen from the laser).

The probing technique was a variant of x-ray absorption near edge spectroscopy (XANES) as in [2] but using the laser-driven backlighter. As the sample is heated, a range of increasing charge states evolves. According to Non-LTE calculations with the PrismSPECT code, the simple L-edge of Cu turns into a multi-step edge when

heated to 10 eV, and new bound-bound absorption features appear; both feature types are temperature-sensitive.

Demonstration of a proton-heated WDM sample and measurement of its temperature history would represent a major step in our ability to create characterized WDM samples for future experiments such as ion stopping measurements with FAIR ion beams.

## Results

### Proton source

The proton spectrum from the main pulse, shown in Figure 2, was measured with a Thomson parabola ion spectrometer and found to extend with a broad distribution typical of TNSA extending up to 7 MeV, corresponding to a range of 350  $\mu$ m in solid Cu.

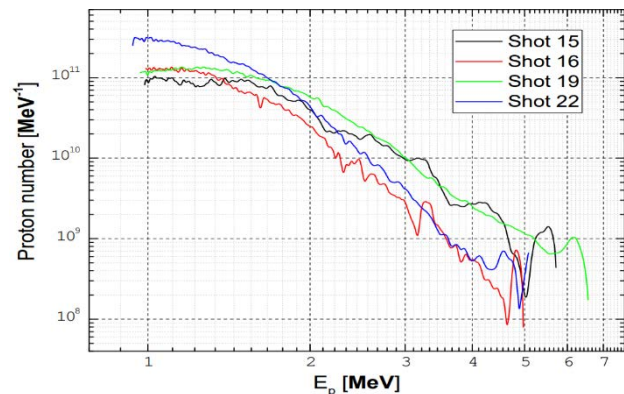


Figure 2: proton spectrum generated by the main split.

### XANES (VSG grating spectrometer)

The spectrometer was calibrated and absorption measurements were made around the Cu L edge and Al K edge at a few delays.

### K-shell emission (HOPG spectrometer)

Ni K- $\alpha$  and K- $\beta$  were observed on all backlighter shots as a monitor. Cu K- $\alpha$  was observed in pump-only and pump + probe shots, while Cu K- $\beta$  was not observed. Further analysis is necessary to derive a temperature minimum value from this fact.

## References

- [1] R. A. Snavely, M. H. Key, S. P. Hatchett, T. E. Cowan, M. Roth, et al., Phys. Rev. Lett. 85, 2945 (2000).
- [2] B. I. Cho, K. Engelhorn, A. A. Correa, T. Ogitsu, C. P. Weber, et al., Phys. Rev. Lett. 106, 167601 (2011).

**Experiment beamline:** none

**Experiment collaboration:** none

**Experiment proposal:** p131

**Accelerator infrastructure:** none

**PSP codes:** none

**Grants:** U.S. Department of Energy Fusion Energy Sciences, High Energy Density Laboratory Plasmas grant DE-SC0014600

**Strategic university co-operation with:** none

# Upgrade of back-reflection diagnostic based on frequency-resolved optical gating at PHELIX\*

*J. Hornung<sup>1,2</sup>, V. Bagnoud<sup>1,2</sup>, M. Zepf<sup>2,3,4</sup>*

<sup>1</sup>GSI, Darmstadt, Germany, <sup>2</sup>Helmholtz-Institut Jena, Germany, <sup>3</sup>Institut für Optik und Quantenelektronik, Friedrich-Schiller-Universität Jena, Germany, <sup>4</sup>School of Mathematics and Physics, Queens University Belfast, UK

## Motivation

During the interaction of an ultra-intense laser pulse with sub-micrometer thin foils, complex effects on the femtosecond timescale take place. During this interaction, a part of the laser pulse is transmitted via hole boring/relativistic transparency and another is reflected back at the position of the critical plasma density. Both the reflected and transmitted pulse are spectrally modulated due to effects like relativistic self-phase-modulation, while the spectrum of the reflected pulse is additionally Doppler-shifted by the moving critical plasma density happening during hole boring. To study these effects and timescales a diagnostic for back-reflected light based on frequency resolved optical gating (FROG) [1] has been developed and implemented at the PHELIX facility [2]. The FROG consists of a single-shot autocorrelator and an imaging spectrometer which spectrally and temporally resolves the incoming laser pulse. To achieve more reliable results the existing diagnostics has been upgraded.

## Upgrade

One part of the upgrade is the change of the spectrometer setup. To keep the device as small as possible, a crossed Czerny-Turner-spectrometer was used in the first setup. Short focal-length mirrors and large reflection angles inside the spectrometer lead to strong aberrations, mostly astigmatism, that strongly influence the spectral resolution and spatial homogeneity of the two-dimensional spectrometer. To reduce the aberrations the focal length of the mirrors has been doubled, from 100 mm to 200 mm and the reflection angles could be reduced from 25 and 20 degree to roughly 16 and 12 degrees. The result of this change can be seen in figure 1, which shows the spectral lines of a calibration lamp.

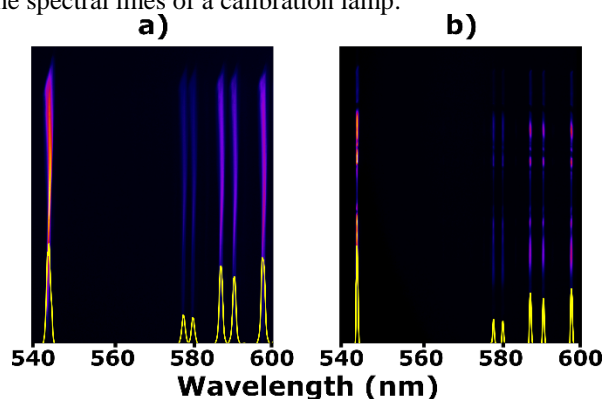


Figure 1: Spectrum of a calibration lamp and the corresponding sum over the complete image in yellow for the old (a) and new (b) spectrometer setup.

The corresponding sum of the spectrum in yellow, for the previous (a) and new (b) configuration, shows narrower lines. This changes the resolution from roughly 1 nm to below 0.5 nm with a much more homogeneous resolution over the whole image.

A further problem, detected during the commissioning of the device, was a slightly asymmetric FROG-trace in the delay axis, shown in figure 2 a), which was due to the misalignment of the autocorrelator and a beamsplitter with a non-equal transmission and reflection ratio. After changing the beamsplitter and realigning the autocorrelator the FROG-trace symmetry in the delay axis could be improved, as shown in figure 2b).

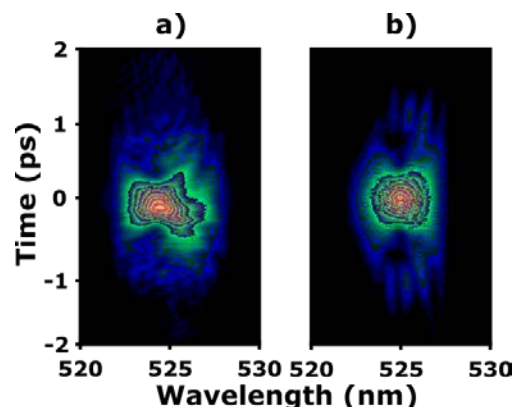


Figure 2: FROG-trace before (a) and after (b) the change of the beamsplitter and realignment of the autocorrelator.

This symmetry improvement increases the accuracy of the pulse-reconstruction algorithm [3] which therefore leads to more reliable measurements.

## Conclusion

The upgrade of the back-reflection diagnostic lead to a more symmetric and spectrally better resolved FROG-trace which will produce more reliable data in upcoming experiments.

## References

- [1] D. J. Kane and R. Trebino, *IEEE Journal of Quantum Electronics* **29**, Issue 2 (1993) 199311
- [2] F. Wagner, J. Hornung, C. Schmidt, et al., *Review of Scientific Instruments* **88** (2017) 023503
- [3] K. W. DeLong, R. Trebino, J. Hunter, et al., *Journal of the Optical Society of America B*, **11** (1994) 002206

\* This report has also been published in "HI-Jena Scientific Report 2017".

**Experiment beamline:** PHELIX  
**Experiment collaboration:** none  
**Experiment proposal:** none  
**Accelerator infrastructure:** none  
**PSP codes:** none  
**Grants:** none  
**Strategic university co-operation with:** Darmstadt

## Generation and transport of heavy ion beams at LIGHT

J. Ding<sup>1</sup>, D. Schumacher<sup>2</sup>, D. Jahn<sup>1</sup>, C. Brabetz<sup>2</sup>, F.E. Brack<sup>3,4</sup>, F. Kroll<sup>3,4</sup>, R. Leonhard<sup>1</sup>, I. Semmler<sup>1</sup>, U. Schramm<sup>3,4</sup>, T.E. Cowan<sup>3,4</sup>, A. Blazevic<sup>2</sup>, V. Bagnoud<sup>2</sup>, M. Roth<sup>1,6</sup>

<sup>1</sup>TU Darmstadt, Darmstadt, Germany; <sup>2</sup>GSI, Darmstadt, Germany; <sup>3</sup>TU Dresden, Dresden, Germany; <sup>4</sup>HZDR, Dresden, Germany; <sup>5</sup>HI Jena, Jena, Germany; <sup>6</sup>FAIR, Darmstadt, Germany

The LIGHT collaboration has been founded to provide a testbed for Laser Ion Generation, Handling and Transport [1]. The laser ion generation is based on the Target Normal Sheath Acceleration (TNSA) mechanism and is driven by the PHELIX 100 TW beam line at GSI. A pulsed solenoid captures and collimates a divergent ion beam coming from the TNSA-driven ion source. By means of chromatic focusing one can cut out a part of the exponentially decaying energy spectrum. The resulting collimated beam can be compressed in phase or energy in a radiofrequency (rf) cavity which is situated two meters behind the ion source. The resulting ion beam is then diagnosed with a diamond detector for a temporal analysis of the achieved phase focus at a distance of six metres from the target.

After a successful first demonstration of the generation, handling and transport of fluorine ions in 2015 [2] and a subsequent campaign in 2016 [3] with small optimizations for the resulting ion beam, two campaigns in 2017 were dedicated to the generation and characterization of a TNSA-driven carbon ion source and the transport and bunching of the resulting ion beam. Figure 1 depicts the energy spectrum of the central part of the carbon ion beam, measured with a Thomson Parabola 0.6 m behind the target.

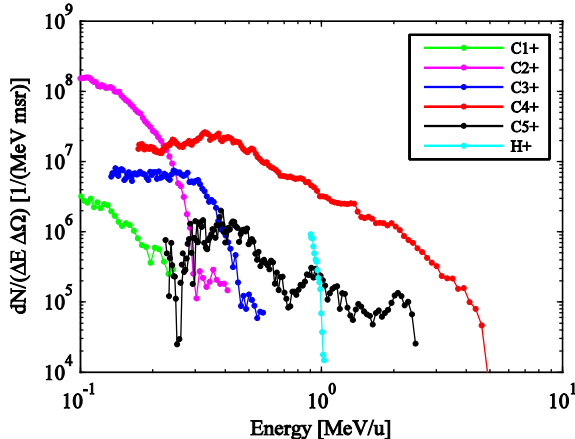


Figure 1: Energy spectrum of TNSA-driven carbon ion source. C4+ dominates the spectrum from 0.5 MeV/u on.

By heating the target up to around 1000 °C one successfully removed most of the hydrogen contaminations on the target surface and enabled efficient acceleration of heavy ions. In the process carbon ions of all charge states, barring 6+, were accelerated together with the remaining hydrogen. From figure 1 it is obvious, that carbon ions with charge state 4+ dominated the beam, from 0.2 MeV/u up to the cut-off energy at around 3.5 MeV/u.

Collimation and transport of the carbon ion beam was achieved with a pulsed solenoid, capable of delivering up to 10 T. From the thin lens approximation in equation (1)

one can derive, that all generated charge states are transported through the beamline at varying energies. With future applications such as energy loss measurements of heavy ions in hot and dense plasmas in mind, the transport energy was set to around 1.2 MeV/u. For this purpose the solenoid was pulsed with 8.92 kA, leading to a maximum magnetic field on axis of 6.72 T.

$$\frac{1}{f} = \frac{q^2}{m^2} \frac{1}{4\gamma^2 v^2} \cdot \int B^2 dz \quad (1)$$

The ion beam was diagnosed with a fast diamond detector. The result is shown in figure 2, where the Time-of-Flight (ToF) data was converted to kinetic energy and the signal has been rescaled due to the related change of bin widths. This also causes a significant rise of the noise level at low ion energies. Simulations with TraceWin, taking space charge into account, show that mainly C4+ was transported with the previously described solenoid configuration and beamline setup. In the simulations the solenoid was modelled as a current-carrying coil. The good agreement of TraceWin simulations with ToF data serves as benchmark for future simulations.

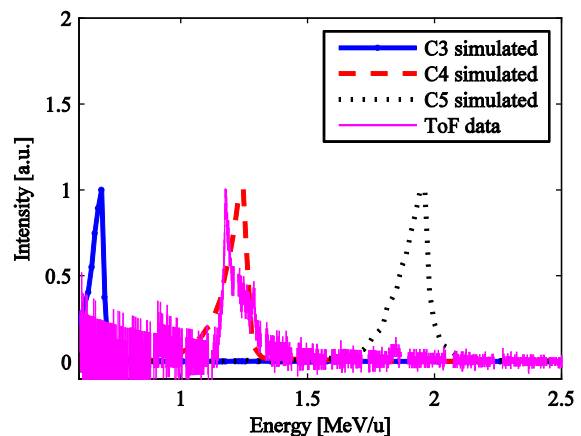


Figure 2: ToF data of diamond detector converted to energy spectrum of transported carbon beam at a solenoid current of 8.92 kA. For decreasing energy the noise per bin increases.

In two successful beam times in 2017, we were able to characterize an efficient TNSA-driven carbon ion source and demonstrate transport and energy collimation of carbon ions in our LIGHT beamline.

### References

- [1] S. Busold et al., NIMA 740, 94-98 (2014).
- [2] J. Ding et al., HEDgeHOB annual report 2015.
- [3] J. Ding et al., HEDgeHOB annual report 2016.

**Experiment beamline:** Z6

**Experiment collaboration:** APPA-HED@FAIR

**Experiment proposal:** I012

**Accelerator infrastructure:** UNILAC other: PHELIX

**PSP codes:**

**Grants:**

**Strategic university co-operation with:**Darmstadt

## Final focussing of collimated proton beams with the laser-driven LIGHT beamline \*

*D. Jahn<sup>1</sup>, D. Schumacher<sup>2</sup>, C. Brabetz<sup>2</sup>, J. Ding<sup>1</sup>, R. Leonhardt<sup>1</sup>, F. Kroll<sup>3,4</sup>, F. E. Brack<sup>3,4</sup>, U. Schramm<sup>3,4</sup>, A. Blazevic<sup>2,5</sup> and M. Roth<sup>1</sup>*

<sup>1</sup>Technische Universität Darmstadt, Darmstadt, Germany; <sup>2</sup>GSI, Darmstadt, Germany; <sup>3</sup>Technische Universität Dresden, Dresden, Germany; <sup>4</sup>HZDR, Dresden, Germany; <sup>5</sup>HI Jena, Jena, Germany.

Laser-driven ion sources offer excellent beam properties (high particle numbers, low emittance) and have been intensely investigated in the past two decades. These sources deliver an exponentially decaying spectrum with a  $\leq 30$  deg divergence. As many applications require a monoenergetic, collimated beam the LIGHT collaboration was founded to combine the advantages of laser-driven ion acceleration with conventional acceleration technology. A prototype beamline has been realized at the Z6 experimental area at GSI [1]. The target normal sheath acceleration source is driven by the Petawatt High-Energy Laser for Heavy Ion Experiments (PHELIX) 100 TW beam and delivers an exponential spectrum up to several tens of MeV. In the next step, a high-pulsed solenoid selects protons of  $(8 \pm 1)$  MeV via chromatic focussing directly 10 cm behind the thin target foil. In 2 m distance, the protons pass a radiofrequency cavity and are phase-rotated. Through the phase rotation the proton bunch can be energy-compressed to  $\Delta E/E_0 = (2.7 \pm 1.7) \%$  or time-compressed into the subnanosecond regime [2]. Behind the cavity, a transport line leads the collimated proton beam to a second target chamber where diagnostics and applications can be placed. Inside this second chamber, a new final focussing system has been installed (6 m behind the target) for steep focussing. This part is necessary to prepare the beam for applications requiring a high intensity beam, e.g. for energy-loss measurements inside plasmas or to study fast processes inside materials. As a final focusing system a second high-field solenoid was placed in the second target chamber and operated at 7 T. As a detector a radiochromic film stack (RCF) was placed 10 cm behind the solenoid. The protons penetrate deeper into the RCF stack, if they have a higher energy according to their characteristic Bragg peak behaviour. The protons deposit their energy inside the RCF films leading to a change in their colour which is analysed. The RCF films of the focus are shown in figure 1. The solenoid parameters have been chosen in this way that 8.3 MeV protons are focussed in a 460 ps bunch length, shown in the 4<sup>th</sup> RCF film (figure 1). The focal spot size is 1.3 mm x 2 mm with  $3 \times 10^8$  protons resulting in a current of  $7.5 \times 10^8$  1/ns  $\sim$  121 mA. The focus profile is shown in figure 2. In 2015, we measured a focal spot size of 2.3 mm x 2.3 mm [3]. In the next experimental campaign in 2018, these focussed proton bunches will be used for first application studies, e.g. precise energy loss measurements in plasma.

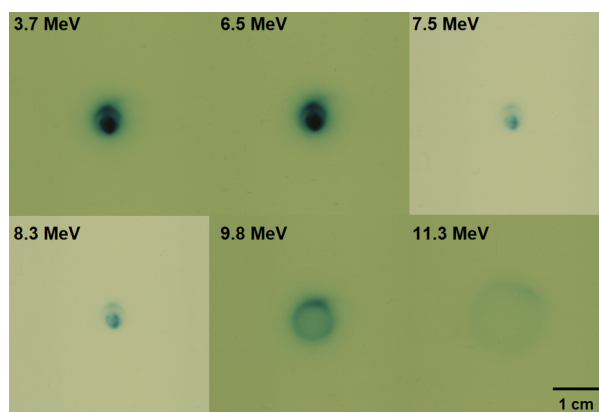


Figure 1: RCF stack detecting the final proton focus: The Bragg peak energy is shown. The 3<sup>rd</sup> and 4<sup>th</sup> RCF films are of the type HD-V2, the others are type EBT3. The solenoid's setting focusses 8.3 MeV protons which is clearly seen in the 4<sup>th</sup> RCF film. On the other RCF films, the particular particle trajectories at the specific energies are shown.

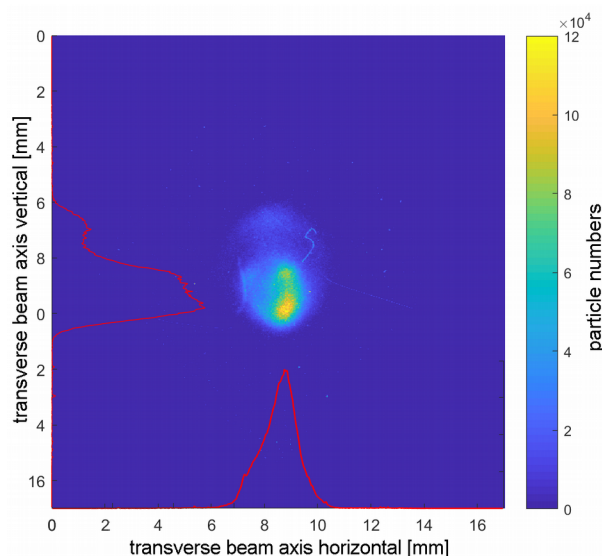


Figure 2: Proton beam profile measured with the 4<sup>th</sup> RCF film: The focal spot size is 1.3 mm x 2 mm at an energy of 8.3 MeV. The deposited energy is converted into particle numbers per pixel and shown.

### References

- [1] S. Busold et al., *NIMA* **740**, 94-98 (2014)
- [2] S. Busold et al., *Scientific Reports* **5**, 12459 (2015)
- [3] D. Jahn et al., *GSI Scientific Report 2015* (2015)

\* This report is also published in *News and Reports from High Energy Density generated by Heavy iOn and Laser Beams 2017*.



**Experiment beamline:** Z6  
**Experiment collaboration:** APPA-HED@FAIR  
**Experiment proposal:** none  
**Accelerator infrastructure:** UNILAC  
**PSP codes:** none  
**Grants:** none  
**Strategic university co-operation with:** Darmstadt

## Emittance measurement with the pepperpot measuring method at the LIGHT beamline

R. Leonhardt<sup>1</sup>, D. Jahn<sup>1</sup>, J. Ding<sup>1</sup>, D. Schumacher<sup>2</sup>, C. Brabetz<sup>2</sup>, F. E. Brack<sup>3,4</sup>, F. Kroll<sup>3,4</sup>,  
U. Schramm<sup>3,4</sup>, A. Blazevic<sup>2,5</sup>, V. Bagnoud<sup>2,5</sup>, and M. Roth<sup>1</sup>

<sup>1</sup>Technische Universität Darmstadt, Darmstadt, Germany; <sup>2</sup>GSI Helmholtzzentrum für Schwerionenforschung, Darmstadt, Germany; <sup>3</sup>Technische Universität Dresden, Dresden, Germany; <sup>4</sup>Helmholtz-Zentrum Dresden-Rossendorf, Dresden, Germany; <sup>5</sup>Helmholtz-Institut Jena, Jena, Germany

The laser-driven LIGHT (Laser Ion Generation, Handling and Transport) beamline at the Z6 experimental area is built to shape ion beams based on the TNSA-source which delivers an exponential spectrum [3]. The ion beam is captured with a solenoid. The solenoid focuses the beam chromatically. The collimated energy is 7.8 MeV with an energy spread of 1.7 MeV. A following rf-cavity enables a phase rotation of the incoming particle beam. The resulting particle pulse length of the particle bunch is  $462 \text{ ps} \pm 40 \text{ ps}$  [1].

Accordingly, the emittance is the central value for the focusability and the divergence of the beam [2]. The used method to measure the emittance is the pepperpot method because it allows the transverse emittance measurement with only one single shot. The pepperpot plate is placed 42.5 cm behind the solenoid. To image the beam behind the pepperpot device radiochromatic films (RCF) are used to image the transported particles which allows to analyze the  $r$ - $r'$  transverse phase space [3]. To analyze the different energies of the particles, the RCF layers are stacked so that the particles with different energies are stopped in different layers of the stack.

In September 2017, latest emittance measurement of a proton beam were performed. First, the solenoid was turned off to measure the emittance of the TNSA-source (fig. 1). Figure 1 shows the RCF image of the TNSA-source at a energy of 3.8 MeV. The picture has the typical pepperpot symmetry. The protons are clustered at specific areas at regular intervals in a two-dimensional array which is seen at the regular dark dots. The transverse emittance of the 3.8 MeV domain is in the x-direction 2.7 mm mrad and in the y-direction 1.5 mm mrad. Figure 2 shows the transverse phase space of the x-direction. The phase space is calculated out of the measured image of figure 1. The transverse phase space of the y-direction is analogous to the phase space of the x-direction.

The next step was to measure the emittance of the focused beam. The solenoid was turned on at different voltages so that the influence of the solenoid voltage on the emittance was measured and will be evaluated in the future.

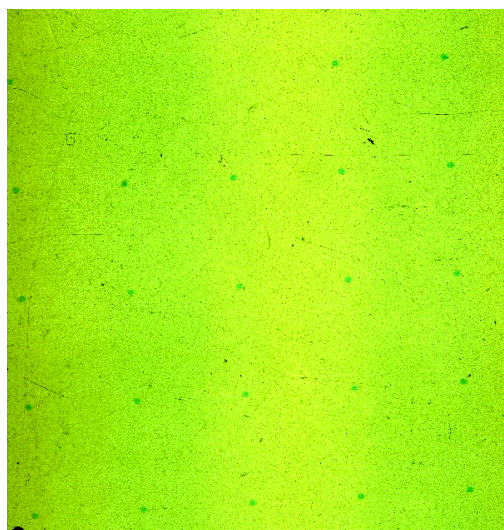


Figure 1: RCF layer at 3.8 MeV showing the TNSA-source emittance. The protons have the beamlet symmetry of the pepperpot, which allows the calculation of each transverse direction of the emittance.

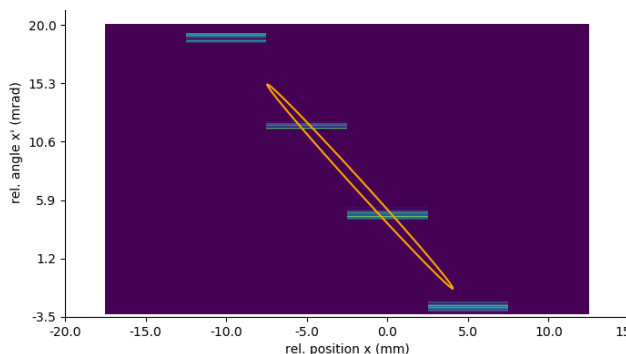


Figure 2: The transverse phase space of the x-direction of the 3.8 MeV domain. The phase space is calculated out of the beamlets in figure 1. The width of the horizontal lines are the angle-distributions of the columns.

### References

- [1] S. Busold et al., Scientific Reports 5, 12459 (2015)
- [2] S. Fritzler et al., Phys. Rev. Lett. 92, 165006 (2004)
- [3] S. Busold et al., Phys. Rev. special topics 16, 101302 (2013)

## Ion acceleration with high laser energy using variable thickness liquid crystal

*P. L. Poole<sup>1</sup>, G. E. Cochran<sup>2</sup>, J. Hornung<sup>3</sup>, V. Schanz<sup>3</sup>, M. Zimmer<sup>3</sup>, V. Bagnoud<sup>4</sup>, M. Roth<sup>3</sup>, B. Zielbauer<sup>4</sup>*

<sup>1</sup>LLNL, Livermore, CA 94551, U.S.A., <sup>2</sup>OSU, Columbus, OH 43210, U.S.A., <sup>3</sup>TU-D, Darmstadt, Germany, <sup>4</sup>GSI, Darmstadt, Germany

Laser-based ion acceleration is an area of significant interest due wide-ranging applications from laboratory astrophysics to radiography to hadron cancer therapy [1]. Several mechanisms have been studied that enable 10s of MeV/nucleon accelerated energies, but the optimization of these depends strongly on both laser parameters (contrast, energy, pulse duration) and target conditions (thickness, density, geometry), requiring multiple campaigns preferably with identical targets.

### Experimental setup

An experimental campaign (Fig. 1) was carried out on the PHELIX laser (180 J, 500 fs, focused intensity  $> 1 \times 10^{20}$  W/cm<sup>2</sup>) to observe changes in accelerated protons due to target thickness variations, achieved with liquid crystal films tunable from 10 nm to over 50  $\mu$ m [2] (inset in Fig. 1). A confocal positioner was used to align the films with  $\mu$ m-scale accuracy, and proton energy was recorded using a stack of RadioChromic Film (RCF). Transmitted light was observed using a Frequency Resolved Optical Gating (FROG) autocorrelator and scatter screen, where enhanced transparency indicates the onset of volumetric acceleration mechanisms.

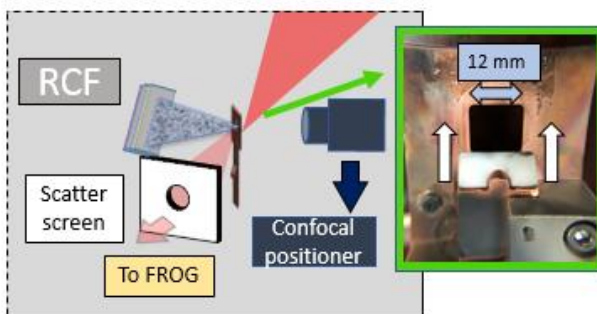


Figure 1: Experimental schematic including target formation device (detail in inset) and several alignment/experimental diagnostics.

### Results and discussion

Though laser fluctuations can significantly impact proton acceleration, the highest RCF dose was observed near 400 nm target thickness for a range of pulse energies (Fig. 2), with a decrease in dose consistently observed for thinner targets. This indicates the onset of laser pre-pulse affecting film morphology prior to main pulse arrival. This data completes a series of liquid crystal ion acceleration experiments [3] taken across 4 facilities with a wide range of

laser energies (1-200 J), pulse durations (30-500 fs), and intensity contrasts, and is the first to be done over this range of parameters using one target material for the full scan.

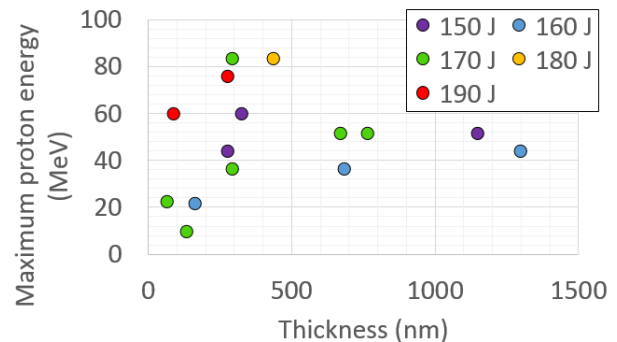


Figure 2: Proton energy observed for changing target thicknesses at different incident laser energies, showing maximum acceleration around 400 nm (error bars  $\pm 3$  MeV).

Properly identifying RCF signal as high energy protons or low energy electrons/x-rays requires a sophisticated stack unfold analysis that is ongoing using data from the set of campaigns. Additionally, 2D Particle-in-cell (PIC) simulations are underway to further understand the intra-target physics inherent to thin target ion acceleration and corroborate the experimental ion data. Figure 3 shows the accelerated proton spectrum from two different intensities on a 250 nm liquid crystal target (implicit solver, energy conserving interpolation, fully ionized target, 12 x 96 nm cell size).

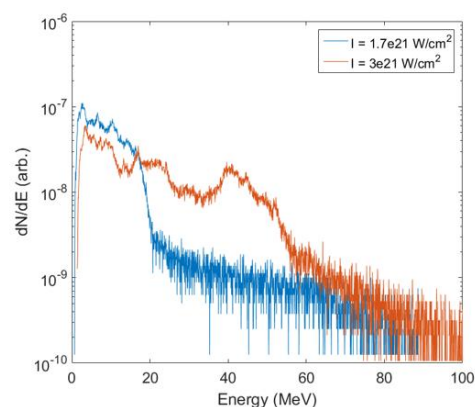


Figure 3: 2D PIC simulation showing proton energy distribution for two different intensities. These simulated spectra can be compared to RCF data to validate proton signal.

### References

- [1] A. Macchi et al., Rev. Mod. Phys. 85, 751 (2013).
- [2] P. L. Poole et al., App. Phys. Lett. 109, 151109 (2016).
- [3] P. L. Poole et al., New J. Phys. 20, (2018).

**Experiment beamline:** none

**Experiment collaboration:** none

**Experiment proposal:** P141

**Accelerator infrastructure:** none

**PSP codes:** none

**Grants:** Euratom research and training programme 2014 - 2018 under grant agreement No 633053; Deutsche Forschungsgemeinschaft through the Munich-Centre for Advanced Photonics cluster of excellence and the program Transregio 18 (TR18)

**Strategic university co-operation with:** Darmstadt

## Ion acceleration using a flattop laser beam

*M. Afshari<sup>1</sup>, V. Bagnoud<sup>1</sup>*

<sup>1</sup>GSI, Darmstadt, Germany;

Laser ion acceleration [1] is of particular interest for Helmholtz Association and for applications driven by upcoming FAIR facilities specifically for warm dense matter studies.

The most widely accepted mechanism for the laser ion acceleration is Target Normal Sheath Acceleration (TNSA) [2]. According to the TNSA model, the shape of the accelerated ions strongly depends on the structure of the hot electron cloud in the backside of the target which itself follows the laser beam profile. Accordingly, a Gaussian laser beam produces a Gaussian hot electron sheath which accelerates ions non-uniformly in all directions. Such high angular distribution is not suitable for most applications due to severe energy loss after passing few micrometers.

In a novel approach we propose a scheme using a phase plate to generate a uniform laser beam which generates a concentrated ion beam with much lower angular divergence. In the following, we present the results of EPOCH [3] simulation for two different laser profiles: first a Gaussian laser profile and second a flattop laser profile to check the differences.

### Gaussian laser profile

To benchmark our simulation, we considered a Gaussian laser profile and simulated its interaction with a 10  $\mu\text{m}$  plastic layer. The laser beam propagates in the x direction and has a peak intensity  $I = 1 \times 10^{21} \text{ W/cm}^2$ , its wavelength equals 1.053  $\mu\text{m}$  and its temporal and spatial lengths equal 575 fs and 8  $\mu\text{m}$  (FWHM) respectively.

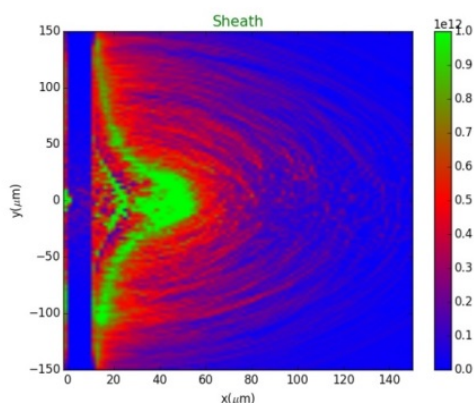


Fig.1: Electrostatic field strength distribution due to the interaction of a Gaussian laser beam with 10  $\mu\text{m}$  plastic.

The interaction of the Gaussian laser profile with the plastic layer creates a Gaussian like sheath, as it is shown in Fig.1 at  $t = 1100 \text{ fs}$ . Such sheath is resulting from not only the laser intensity distribution but also the electron dynamics at the rear side of the target. For these simulation parameters, the angular distribution of the protons found to be a typical TNSA angular distribution with a divergence angle with the FWHM of  $50^\circ$ .

### Flattop laser profile

The novel idea of this study is to work with a distribution of the laser focus that is spatially top hat. A way to come around this difficulty is to employ a random phase plate (RPP) that creates a speckle pattern of high spatial frequency over the desired spot size. The laser propagates in the x direction and has peak intensity  $I = 1 \times 10^{19} \text{ W/cm}^2$ , wavelength equals to  $\lambda = 1.053 \mu\text{m}$  with temporal and spatial lengths equal to 1000 fs and 104  $\mu\text{m}$  (FWHM) respectively. The electric field distribution at the input of the simulation box is calculated using Matlab such as to obtain the desired intensity distribution at  $x = 0$  and fed as numerical input into EPOCH. Using the same laser parameters, energy and duration, as for the Gaussian beam yields reduced electrostatic field strength, as it can be seen in Fig.2, but the resulting electric field distribution is much more favourable. Indeed, the interaction of the flattop laser profile with the 10  $\mu\text{m}$  plastic target creates a smooth and uniform flattop sheath which propagates in the direction normal to the target. The most important result is that the angular distribution of ions now is much more peaked around the target normal direction. At this instant, the particles are propagating in a total divergence angle of  $12^\circ$  with the FWHM of  $2^\circ$ .

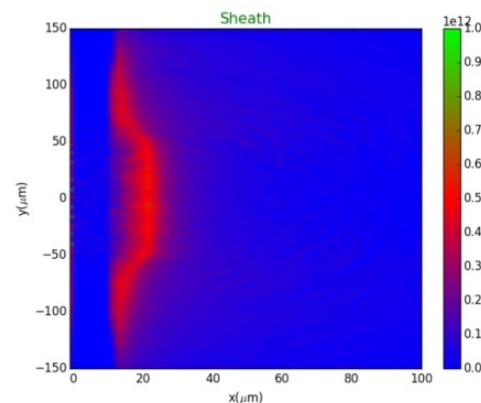


Fig.2: Electrostatic field strength distribution due to the interaction of a flattop laser beam with 10  $\mu\text{m}$  plastic.

### References

- [1] M. Roth et al., The generation of high-quality, intense ion beams by ultra-intense lasers, *Plasma Phys. Control. Fusion*, 44 (2002).
- [2] S. C. Wilks et al., Energetic proton generation in ultra-intense laser–solid interactions, *Physics of Plasmas*, 8, 542 (2001).
- [3] T. D. Arber et al., A particle-in-cell code for laser-plasma interactions: test problems, convergence and accuracy, *J. Comp. Phys.*, 2014.

**Experiment beamline:** none  
**Experiment collaboration:** APPA-HED@FAIR  
**Experiment proposal:** P152  
**Accelerator infrastructure:** other: PHELIX  
**PSP codes:** none  
**Grants:** Euratom EUROfusion-ER-ToIFE(19040)  
**Strategic university co-operation with:** none

## Progress on the development of an actively cooled glass amplifier at PHELIX

M. Patrizio<sup>1</sup>, V. Bagnoud<sup>2,3</sup>, B. Zielbauer<sup>2</sup>, M. Roth<sup>1,4</sup>

<sup>1</sup>TU Darmstadt, Darmstadt, Germany; <sup>2</sup>GSI, Darmstadt, Germany;

<sup>3</sup>Helmholtz-Institute Jena, Jena, Germany; <sup>4</sup>FAIR, Darmstadt, Germany;

As contribution to FAIR, PHELIX, in cooperation with the Technical University of Darmstadt and funded by the Bundesministerium für Bildung und Forschung (BMBF), is developing an actively cooled glass amplifier for a PHELIX-like laser system planned as a diagnostic tool at the APPA Cave at FAIR. This new amplifier design seeks to improve on the repetition rate of glass disc laser systems to enable more elaborate experimental campaigns [1].

### Simulated wave front deformation

Building on the simulations discussed in [2], a mesh containing the temperature distribution in the glass discs can be exported. Taking into account the temperature induced change in refractive index and expansion of the glass this temperature mesh can be converted into a 2D map of the optical path length. From this map the deformation of a plane wave transmitted through the amplifier glass can be calculated (Fig. 1). The simulation results show very low phase deformations after 300 s of cooling. This further encourages development of the concept.

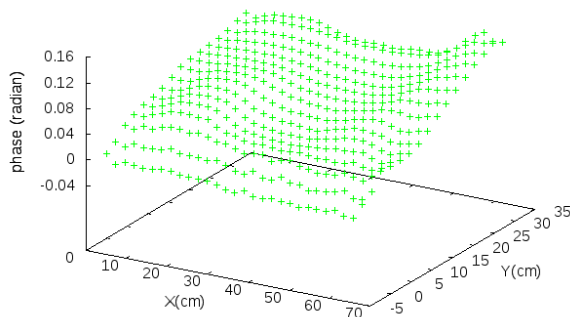


Figure 1: Simulated wave front behind the amplifier after a cooling time of 300 seconds.

### Cooling liquids

Extensive research was conducted to find a suitable cooling liquid for our amplifier. During this research several key parameters of the potential coolants have been identified. Refractive index, absorption coefficient, viscosity and chemical compatibility are the most important factors to be taken into account. The heat capacity is negligible due to the low thermal conductivity of the glass. Since the absorption coefficient for liquids at certain

wavelengths is not readily available for many liquids, help was acquired from the department of Surface chemistry and spectroscopy at the Technical University of Darmstadt. Their Photo-Spectrometer was used to measure the absorption coefficients for several potential cooling liquids. This was done to assess the viability a perfluorinated hydrocarbons (F2 PP-series). The results are shown in Fig. 2.

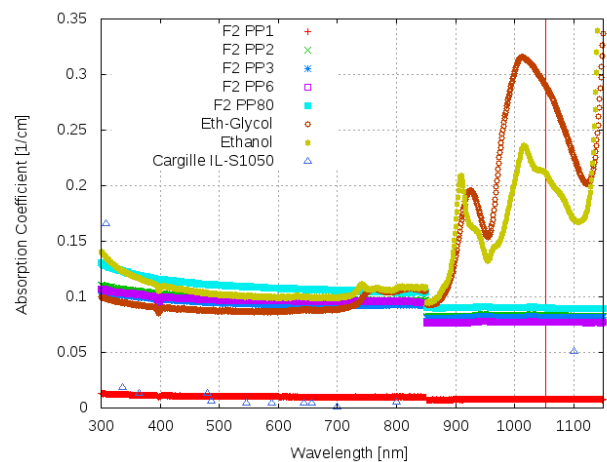


Figure 2: Absorption coefficients of several potential cooling liquids as function of their wavelength (laser wavelength as red vertical line). Measurements conducted at TU Darmstadt, Workgroup Prof. Dr. Hess. Data for Cargille IL-S1050 extracted from data sheet for reference.

### Concept Design

Parallel to the search for a suitable cooling liquid the design phase for a concept of the amplifier prototype was started. The concept calls for a modular design for various configurations of the prototype, compatibility with the PHELIX infrastructure for potential Phase-0 use, no contact between glass and metal parts to avoid damaging the glass and no bending forces on the glass especially in the direction of the laser beam to avoid additional distortions of the wave front.

### References

- [1] V. Bagnoud *et al.*, Laser-based pump-probe equipment for the APPA Cave at FAIR, Revision 2.2 (2014) (TDR for the HEDgeHOB/WDM collaborations at FAIR)
- [2] M. Patrizio *et al.*, Development of an actively cooled glass amplifier at PHELIX, GSI Scientific Report 2016 (DOI:10.15120/GR-2017-1)

## Stretcher simulation for temporal laser pulse profile optimization

V.A. Schanz<sup>1,2</sup>, V. Bagnoud<sup>1</sup>, M. Roth<sup>2</sup>

<sup>1</sup>GSI, Darmstadt, Germany; <sup>2</sup>TU Darmstadt, Darmstadt, Germany

The temporal pulse profile of a high-intensity laser pulse is very relevant for laser-plasma experiments. Parts of the pulse interacting with a target are already intense enough to create a pre-plasma prior to the arrival of the main peak. The rising slope of the laser pulse, which persists hundreds of picoseconds, influence the pre-plasma conditions the most. Several publications in the past conclude noise in the CPA-systems stretcher as the prime reason for this slow rising slope. For further investigation, we developed a MATLAB based ray tracing code, simulating stretcher geometry with the possibility to generate noise at the optics of the stretcher. In this report, we present the status quo of this ray tracing simulation.

### Temporal pulse contrast

Up to the present day, all short-pulse high-intensity laser systems have one issue in common: the need to improve and understand their temporal contrast, which is defined as the ratio of the maximum intensity to the intensity of the pulse at a certain time before the maximum. Especially, the rise time at the leading edge of the main peak, which is depicted in Figure 1, is much longer than a Fourier-transform limited pulse dictates.

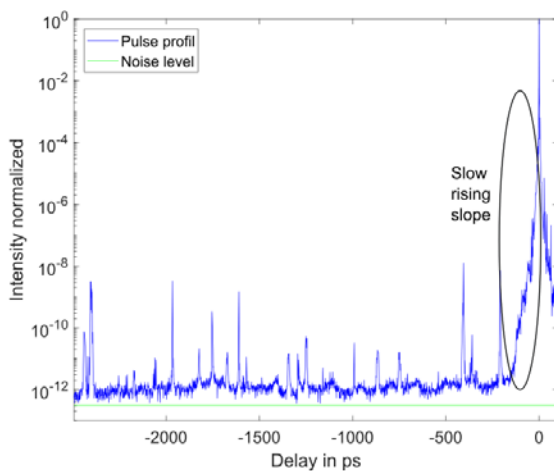


Figure 1: Temporal pulse profile of the PHELIX laser, measured with a specially designed detector [1,2]. The detection limit is shown in green and the leading edge, which will be improved with the development presented in this report, is highlighted in black.

Almost all high-intensity short-pulse laser systems are based on the chirped pulse amplification (CPA), where the pulse is temporally stretched, amplified and afterwards recompressed. Stretching and compression are done by the arrangement of dispersive optics, e.g. gratings, whereby a wavelength dependent optical path is achieved. Today's conventional wisdom expects the main reason for the shape of the leading slope in amplitude and phase modulations, occurring in the stretcher.

### Ray tracing CPA system analysis

To investigate this topic, we created a MATLAB based ray tracing code and simulated the propagation of a beam through a stretcher-compressor setup (Fig. 2), resulting in zero dispersion after propagation through the whole system.

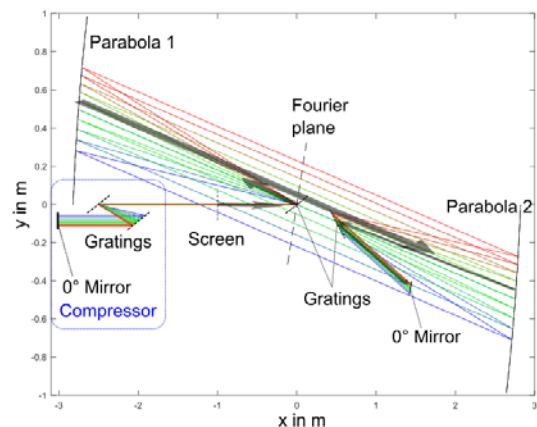


Figure 2: Visualization of a simulated beam path, generated with a self-written ray tracing code. Different colours represent beams with different wavelength. Positions of simulated optics and for calculation needed planes (Screen and Fourier plane) are shown in black. Rays start at the screen, propagating to the right, following the indicated grey arrows. After hitting the 0° mirror, they propagate back on the same path, passing the screen and entering the compressor. For clarity reasons, no arrows are shown for the second pass (back) in the stretcher and the passes in the compressor.

Randomly distributed scattering objects, with densities corresponding to clean room definitions, are defined on the gratings and the Fourier plane. When hit, such an object will attenuate the intensity of an incoming ray and apply an additional phase. At a defined screen the spectrum and spectral phase of the resulting pulse after propagation through the system is determined. This allows the calculation of the resulting temporal pulse profile.

Parameter studies will be carried out this year to investigate the influence of different distortions at different optics, followed by experimental verification.

### References

- [1] V.A. Schanz et al., "Noise reduction in third order cross-correlation by angle optimization of the interacting beams", *Opt. Express* 25, 9252-9261 (2017)
- [2] V.A. Schanz et al. EP 16 188 142.0, EPO, patent pending

Strategic university co-operation with: Darmstadt



## Characterization of hard X-ray sources for radiographic purposes at the PHELIX laser

B. Borm<sup>1</sup>, J. Hornung<sup>2</sup>, D. Khaghani<sup>2,3</sup>, P. Neumayer<sup>4</sup>

<sup>1</sup>Goethe-Universität Frankfurt, Germany; <sup>2</sup>Helmholtz-Institut Jena, Germany; <sup>3</sup>Friedrich-Schiller-Universität Jena, Germany; <sup>4</sup>GSI, Darmstadt, Germany

High-energy high-intensity lasers – like the Petawatt Laser for Heavy Ion Experiments (PHELIX) at GSI – are a formidable tool to create hard X-ray sources with extraordinary properties. These are mainly the short emission duration, which is in the same order of magnitude as the laser pulse duration, the small source size, which is defined by both the target geometry and the laser focus size, and the spectral distribution which extends into the several 100 keV range [1]. All of these properties make laser-based hard X-ray sources very suitable for radiography of hydrodynamically evolving high-Z high-density plasmas, like they will be produced in the future plasma physics experiments at FAIR (e.g. LAPLAS). Since the emitted X-ray spectrum depends on a variety of experimental parameters, particularly the laser intensity and the target geometry, a full characterization of the source properties is an appropriate step to reliably predict radiographic imaging performance.

We have performed an experiment at the PHELIX laser with the goal to determine the emission characteristics of bremsstrahlung X-ray sources regarding spectral and angular distribution, depending on the laser intensity and contrast and on the target geometry. Furthermore, the source sizes were measured. The laser intensity was varied between  $4.1 \times 10^{16}$  and  $1.1 \times 10^{20}$  W/cm<sup>2</sup>, the contrast between the “low” of  $10^{-6}$  and the high of  $<10^{-10}$ . Two target types were used: gold foils of 5  $\mu\text{m}$  thickness and tungsten wires of 5  $\mu\text{m}$  diameter. Bremsstrahlung was detected by a set of 12 hard x-ray spectrometers, placed in the horizontal and vertical around the target (white tubes in Fig. 1). Using imaging plate detectors and a set of tantalum filters, the spectrometer working range is 20-400 keV. The attenuated signal was fitted by a Maxwellian energy distribution with two effective temperatures to retrieve conversion efficiencies (CEs) from laser energy to

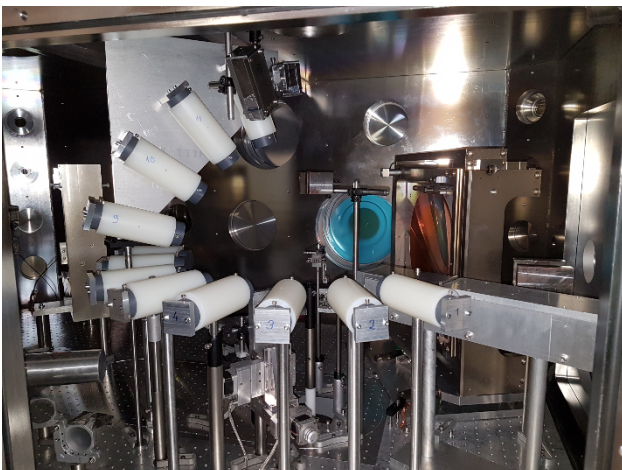


Figure 1: Hard x-ray spectrometer array to determine the emission distribution of the laser-driven x-ray source.

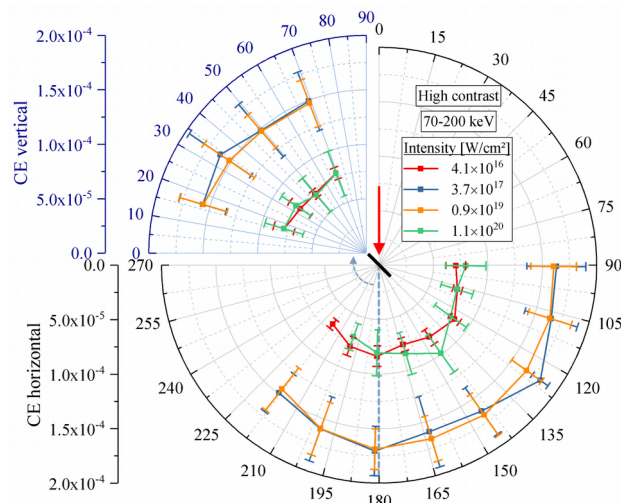


Figure 2: Angular dependency of the CE

x-ray emission into the 70-200 keV range. Source sizes were determined using a gold knife-edge imaging setup with 1  $\mu\text{m}$  spatial resolution.

We find that bremsstrahlung up to 400 keV is emitted isotropically, independent of laser intensity and contrast (see Fig. 2) and target type. The CE however rises between the lower two intensities used, then drops again for the highest by a factor of around 2. The CE is systematically higher for the low contrast laser pulses by up to a factor of 2. On average, we determined a CE into the 70-200 keV interval of  $(1.5 \pm 0.2) \times 10^{-4}$  at  $0.9 \times 10^{19}$  W/cm<sup>2</sup> and high contrast using gold foil targets.

The source sizes measured in the thin direction of the foil targets varied between 3.7-12.0  $\mu\text{m}$ . On average, wire targets at high contrast showed 5  $\mu\text{m}$  source size, exactly their diameter. In a follow-up experiment, this laser-generated x-ray source has enabled x-ray phase contrast imaging of laser-driven shock waves.

### References

- [1] R. Tommasini *et al.*, Physics of Plasmas. **18**, 056309 (2011)
- [2] L. Antonelli *et al.*, GSI Scientific Report 2017

**Experiment beamline:** PHELIX  
**Experiment collaboration:** none  
**Experiment proposal:** P134  
**Accelerator infrastructure:** none  
**PSP codes:** none  
**Grants:** none  
**Strategic university co-operation with:** Frankfurt-M

## Application of a TLD-based ten channel system for the spectrometry of bremsstrahlung generated by laser-matter interaction

N. Zahn<sup>1</sup>, O. Rosmej<sup>1,2</sup>, F. Horst<sup>2</sup>, S. Zähler<sup>1</sup>, A. Sokolov<sup>2</sup>, N. Borisenko<sup>3</sup>, L. Borisenko<sup>3</sup>, N. Pimenov<sup>4</sup> and J. Jacoby<sup>1</sup>

<sup>1</sup>Goethe University, Frankfurt, Germany; <sup>2</sup>GSI, Darmstadt, Germany; <sup>3</sup>P. N. Lebedev Physical Institute (RAS), Moscow, Russia; <sup>4</sup>Zelinsky Institute of Organic Chemistry (RAS), Moscow, Russia

The interaction of relativistically intense laser pulses produced by the PHELIX-system with near critical plasmas has been investigated in order to optimize the energy and the total charge of the laser-accelerated electron bunch for FAIR-relevant applications. The enormous increase of total charge and energy of the laser-accelerated electrons was predicted by the theory [1], that is much higher than defined by Wilks law [2]. In described experiments, electrons were accelerated in plasma of near critical density. The electron energy distribution was directly analysed by applying a static magnetic field and indirectly by measuring the bremsstrahlung radiation produced when MeV electrons were passing through the 17 mm-thick steel flange placed 87 cm distant from the target in the laser propagation direction. For measurements of the gamma bremsstrahlung spectra 10 channels TLD detector-based thermoluminescence dosimetry method was applied.

The schematic drawing of the ten channel spectrometer is shown in Fig. 1. The TLD-spectrometer has a cylindrical shape with a default incident direction of the radiation. Ten TLD-cards are placed between absorbers of different material and thickness inside a shielding from lower to higher Z materials with a collimator window in the front. The incident x-rays penetrate the TLD's. The absorbers cause a different response of every TLD, which can be used as information about the spectrum of the incident x-rays. The spectrometer is designed for an energy range from 30 keV to 100 MeV [3].

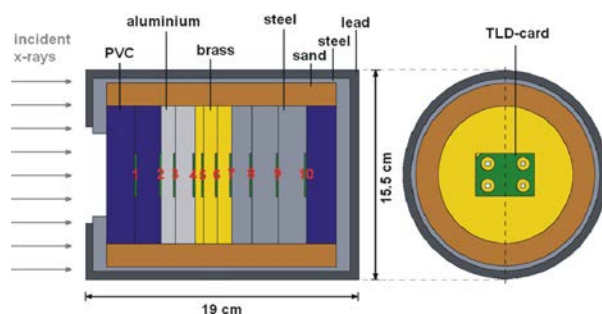


Figure 1: Schematic view of the TLD-spectrometer [3].

The materials of the TLD cards used in these measurements are pieces of doped lithium fluoride in two variations - Harshaw TLD 700 (<sup>7</sup>LiF: Mg, Ti) and TLD 700H (<sup>7</sup>LiF: Mg, Cu, P). TLDs absorb radiation and emit photons proportionally to the deposited dose when heated to a few hundred degrees Celsius.

In the experiment (P138, Oktober 2017) electrons were accelerated in the interactions of the PHELIX-laser pulse of  $3 \cdot 10^{19}$  W/cm<sup>2</sup> intensity with different foil-targets (Ti, Cu, Ta) of 5-20  $\mu$ m thickness and with low density foams. Additionally, foil-targets were combined with the CHO

foam layer (2mg/cc Triacetate-Cellulose C<sub>12</sub>H<sub>16</sub>O<sub>8</sub>) with thickness of 300 and 500  $\mu$ m. The laser energy was 100 J, with pulse duration of  $750 \pm 250$  fs. Supplementary to the shots with a single laser pulse, a double pulse configuration was used where a 1.5 ns prepulse with a time delay of 0.5-3 ns before the main pulse and energies of 1-3 J was applied in order to drive a super-sonic ionization in the low density CHO-foams and create a homogeneous channel of near critical plasma. Using pre-ionized by the ns-prepulse low-density CHO-plasma with a mean density near to the PHELIX-laser critical density ( $n_e = 10^{21}$  cm<sup>-3</sup>) it was possible to increase by 2-3 orders of magnitude the fraction of 20-100 MeV electrons compared to the case of the laser interaction with planar foils and thus to gain 2-3 orders of magnitude increase of the gamma-rays. Preliminary results for the spectrometer response to different laser shots are shown in Fig. 2. The experiments have shown the effective generation of electrons with tens of MeV-energy if the relativistic laser pulse interacts with extended plasmas of the near critical density.

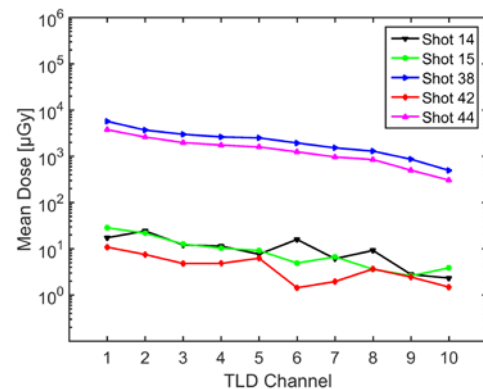


Figure 2: Preliminary results for five different shots. Shots 14, 15 and 42: contrast  $10^{-10}$ , no prepulse, target – 25  $\mu$ m Cu-foil. Shots 38 and 44: contrast  $10^{-10}$ , prepulse – 1 J,  $t = 1.5$  ns,  $dt = 5$  ns, target – CHO-Foam 500  $\mu$ m.

The main mechanisms leading to extreme high electron energies are the laser beam self-focusing in the pre-plasma and a betatron mechanism of the electron acceleration. TLD measurements of the radiation dose are consistent with results of the electron spectrometers. Using the Monte Carlo code FLUKA [4] the electron spectra will be evaluated from the photon radiation doses measured by the TLDs.

### References

- [1] L. P. Pugachev et al., NIM A **829** (2016) 88-93.
- [2] S. C. Wilks et al., Phys. Rev. Lett. **69** (1992) 1383.
- [3] F. Horst et al., NIM A **782** (2015) p. 69-76.
- [4] <http://www.fluka.org>.

## Optimisation of laser based sources of electrons and gammas for backlighting of high areal density targets at FAIR\*

Ş. Zähler<sup>1</sup>, O. Rosmej<sup>2</sup>, N. Andreev<sup>3</sup>, L. Borisenko<sup>4</sup>, N. Borisenko<sup>4</sup>, B. Borm<sup>1,2</sup>, P. Christ<sup>1</sup>, F. Horst<sup>2,5</sup>, P. Neumayer<sup>2</sup>, D. Khaghani<sup>2,6</sup>, V. Pimenov<sup>7</sup>, L. Pugachev<sup>3</sup>, K. Schmal<sup>1</sup>, C. Wagner<sup>1</sup>, N. Zahn<sup>1</sup>, K. Zerbe<sup>1</sup>, J. Jacoby<sup>1</sup>, APPA-HED@FAIR, Plasmaphysics/PHELIX

<sup>1</sup>Institute for Applied Physics (IAP), Goethe University, Frankfurt am Main, Germany; <sup>2</sup>GSI, Darmstadt, Germany; <sup>3</sup>Joint Institute for High Temperatures (JIHT), Russian Academy of Sciences (RAS), Moscow, Russia; <sup>4</sup>Lebedev Physical Institute (LPI), RAS, Moscow, Russia; <sup>5</sup>Justus-Liebig-University, Giessen, Germany; <sup>6</sup>Friedrich Schiller University, Jena, Germany; <sup>7</sup>Zelinsky Institute of Organic Chemistry (ZIOC), RAS, Moscow, Russia

The development of laser based intense and well directed beams of MeV electrons and Gamma-rays for backlighting states of matter with high areal density is of great importance for the planned experiments at FAIR. If the laser parameters cannot be changed, one will be able to optimise the properties of the secondary laser sources using custom made structured targets of near critical density. A significant increase of the electron number at tens of MeV energy makes such type of laser-based electron source very prospective for the diagnostic of high areal density high energy density states. Simulations demonstrate that the interaction of relativistic laser pulses ( $2 - 4 \cdot 10^{19} \text{ W/cm}^2$ ) with a near critical plasma layer ( $10^{21} \text{ cm}^{-3}$ ) leads to an effective generation of highly energetic electrons ( $>10\text{-}20 \text{ MeV}$ ), carrying a charge that at least 2 orders of magnitude exceeds prediction by ponderomotive scaling for the incident laser amplitude [1]. Electrons accelerated from the by a ns-prepulse preionised low density foam target (triacetatecellulose,  $\text{C}_{12}\text{H}_{16}\text{O}_8$ ) with a thickness of  $500 \mu\text{m}$  and  $2 \text{ mg/cm}^3$  density have the highest energies and the highest charge (ca.  $25 \text{ nC}$  for electrons with energies higher than  $30 \text{ MeV}$ ). In this work we present first pilot experiments on the characterization of MeV electron beams generated by the interaction of the PHELIX-laser pulse with low density CHO-foams (P138, October 2017).

Electron spectra up to  $100 \text{ MeV}$  were measured by the application of dipole magnets as dispersive elements. The electrons follow a certain path in the spectrometer according to their kinetic energy and the radius of gyration. That leads to a calculated dispersion. FUJI Film BAS-TR imaging plates were used as detectors. The response function of the imaging plates is known for photons, electrons and several types of heavier particles [2]. The schematic of this electron spectrometer is shown in Figure 1.

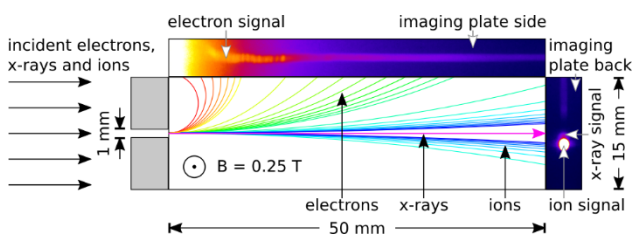
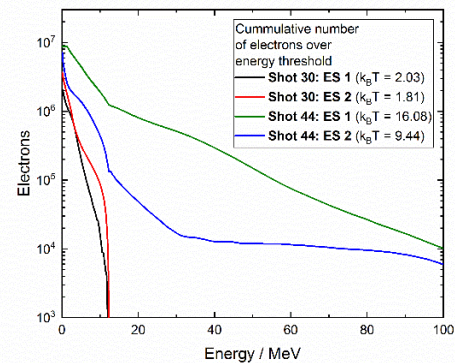


Figure 1: Schematic view of the electron spectrometer. Data shown in false colour images.

The interaction of the high power laser pulse of relativistic intensities with different target materials allow for the generation of MeV electrons. The Ponderomotive law

predicts an electron temperature of  $2.1 \text{ MeV}$  for the used laser intensity. In the mentioned experiments with near critical plasmas the production of intense MeV electron beams is demonstrated. Figure 2 shows the cumulative number of electrons above an energy threshold up to  $100 \text{ MeV}$ . The usual way for laser-based particle acceleration is to shoot onto Cu-foils (shot 30, black and red solid lines). In comparison the interaction of relativistic laser pulses with pre-ionized low density plasmas of near critical density leads to a strong increase of the number of



electrons with energies above  $10 \text{ MeV}$  (green solid line, shot 44).

Figure 2: Cumulative number of electrons above energy threshold.

Electrons are mostly accelerated in laser direction reaching a mean energy/temperature of  $16 \text{ MeV}$ . Hot MeV electrons interacted with a  $17 \text{ mm}$  thick Fe-flange and created hard bremsstrahlung radiation measured by means of a 10 channel TLD-spectrometer [3]. The radiation dose on the TLD-cards showed the same result as the electron spectrometers: 2-3 orders of magnitude increase in the bremsstrahlung dose for the direction of laser propagation. The experiments have demonstrated the stability of the effect.

## References

- [1] L.P. Pugachev et al., "Acceleration of electrons under the action of petawatt-class laser pulses onto foam targets", NIM A 829 (2016), pp. 88-93.
- [2] T. Bonnet et al., "Response functions of imaging plates to photons, electrons and  $4\text{He}$  particles", RSI 84 (2013), pp. 103510-1-103510-7.

- [3] F. Horst et al., "A TLD-based ten channel system for the spectrometry of bremsstrahlung generated by laser-matter interaction", NIM A (2015), p. 1.

**Experiment beamline:** PHELIX

**Experiment collaboration:** APPA-HED@FAIR

**Experiment proposal:** P138

**Accelerator infrastructure:** none

**Grants:** BMBF-Project: 05P15RGFAA, HGS-Hire

**Strategic university co-operation with:** Frankfurt-M / Gießen

---

\* Work supported by BMBF-Project: 05P15RGFAA, HGS-Hire;  
This report is also submitted to "News and Reports from High Energy  
Density generated by Heavy Ion and Laser Beams 2017"

## Investigation of proton induced demagnetisation effects in Permanent Magnet Quadrupoles\*

M. Endres<sup>2</sup>, M. Schanz<sup>1,2</sup>

<sup>1</sup>GSI, Darmstadt, Germany; <sup>2</sup>TU Darmstadt

The PRIOR-I (Proton Microscope for FAIR) proton microscope at the GSI experimental area HHT employs a system of permanent magnet quadrupoles (PMQs) for imaging using protons from the SIS-18 accelerator [1]. After the first tests with this particular prototype, the demagnetisation of these PMQs due to primary and secondary radiation was investigated. Therefore, a spare module consisting of several magnetic wedges forming a Halbach Array-type Quadrupole [2] was deliberately irradiated.

### Measuring the magnetization direction

In order to measure the hysteresis loops of the irradiated material, samples were cut out of the single wedges. The measurement itself was carried out with a pulsed field magnetometer (Metis HyMPulse)† where the magnetization direction of the outer applied field of the magnetometer has to be parallel to the internal field of the sample. This means the surface of the cut sample and the direction of the magnetization  $\alpha$  have to be parallel. A misalignment could lead to a steep inclination in the flat top region of the loop. The first measurements showed exactly this behaviour. To improve the results, a method for the determination of  $\alpha$  was developed.

A measurement was set up to determine the inclination of the magnetic field at the surface of the wedges. The wedges were scanned with a 1D Hall sensor by the magnet department of GSI. On a path of 30 mm first the  $B_x$  component was measured then the sensor was turned by  $90^\circ$  to measure the  $B_y$  component. This was done on the upper and the lower side of the Wedge.

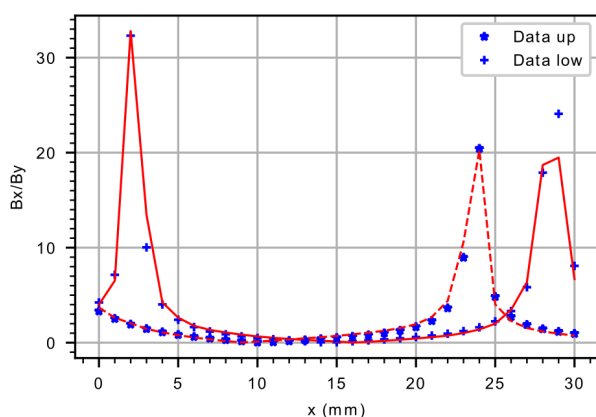


Figure 1: The inclination of the magnetic flux on the lower (full) and upper (dashed) surface of wedge 10 with the best fitting simulation.

This data was compared to simulations [3] of the field of the wedges for different directions of the magnetisation. A fitting routine selected the best fitting pattern of inclinations. With this procedure the magnetisation direction could be determined. For example the magnetization angle of wedge 10 (see Figure 1) was found to be  $\alpha \approx 82.5^\circ$ . According to the specification it should be  $75^\circ$ . The measured direction differed approximately 7.5 degrees from the specified angles.

### Degradation of the HD5 value

Using the known deviations of the magnetization directions the hysteresis loops of different irradiated wedges were measured again. The HD5 value was chosen as a benchmark for the amount of demagnetization. It is given by the intersection of the hysteresis loop itself with 90% of a straight line fitted to the flat top part of the loop. A degradation of the material due to radiation leads to a decreased stability towards a demagnetizing field. This in turn leads to a larger bending of the left section of the loop which also results in a lower HD5 value.

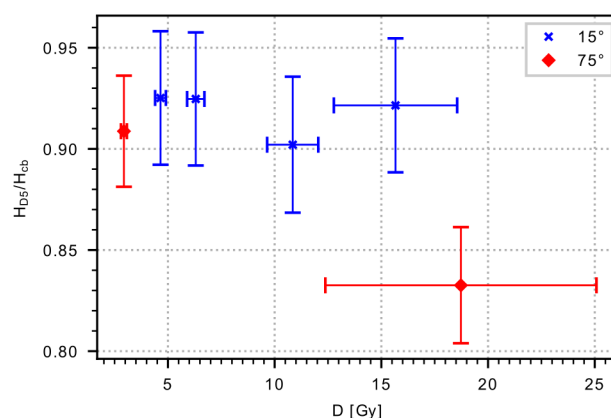


Figure 2: The HD5 values versus the applied dose recorded with Gafchromic films for different segments [4]

The analysis of the hysteresis loops for different wedges revealed that wedges containing a higher internal demagnetization field (type  $75^\circ$ ) showed a significantly larger degradation of the HD5 value than the wedges from regions with a lower internal demagnetization field (type  $15^\circ$ ). These results and further investigations on the origin of the observed damage were already published [4].

\* Work supported by BMBF (05K13RDB). This report is also submitted to “News and Reports from High Energy Density generated by Heavy Ion and Laser Beams 2017”

† Measurements by K. Löwe (Group Functional Materials, TU Darmstadt)

**Reference**

- [1] D. Varentsov et al, Rev. Sci. Instrum. 87, 023303 (2016)
- [2] K. Halbach, Nucl. Instru. Methods 169,1 (1980)
- [3] Finite Elements Methods Magnetics (FEMM), Version 4.2, www.femm.info (October 2010)
- [4] M. Schanz et al, Rev. Sci. Instrum. 88, 125103 (2017)

**Experiment beamline:** SIS18-other: HHT

**Experiment collaboration:** APPA-HED@FAIR

**Accelerator infrastructure:** SIS18

**Grants:** BMBF (05K13RDB)

**Strategic university co-operation with:** Darmstadt

## On equation-of-state measurements at the binodal in ion-beam heated matter

An. Tauschwitz<sup>1</sup>, O. Rosmej<sup>2</sup>, A. Tauschwitz<sup>2</sup> and J. Jacoby<sup>1</sup>

<sup>1</sup>Institute for Applied Physics, Goethe University Frankfurt, Germany; <sup>2</sup>GSI, Darmstadt, Germany

Modern particle accelerators provide intense beams of energetic charged particles which are able to create extended samples of matter at high energy density. The experimental area HHT at the SIS-18 heavy ion synchrotron allows to use focused ion beams of moderate intensities which means that a careful choice of beam-target configuration is essential to obtain meaningful experimental data. In the past it was proposed to heat isobarically a low density foam with energetic heavy ions to investigate the phase diagram and critical point parameters of selected materials [1]. Later on, the behaviour of a single foil heated initially at constant pressure and then undergoing a transition to the liquid-gas equilibrium state was described in [2].

In this second approach, shown schematically in Fig. 1, the expansion starts at the point  $O$  at the cold curve and follows the metastable EOS along an isobar. If the condition of quasi-static isobaric expansion is fulfilled, i.e. the foil is thin enough for a given heating rate, then, to a good accuracy, all thermodynamic quantities are constant in space and the entire foil is represented by a point on the phase plane. The expanding foil crosses the binodal in the liquid state at point  $B_0$  and, before approaching the spinodal, undergoes a practically instantaneous transition into a gas-liquid equilibrium:  $B_1 \rightarrow B_2$ . The exact moment of vaporization of the metastable liquid inside the binodal curve is determined by the criteria of explosive boiling [2]. For sufficient beam power deposition the expansion after the transition is no longer isobaric. The reason for this is the lower sound speed in the liquid-gas mixture compared to the pure liquid. Hence, the different fluid elements follow different phase trajectories after the transition. At figure 1 the lower curve starting at point  $B_2$  corresponds to the foils surface relaxing quickly to ambient pressure  $p_0$ . The upper curve represents the foil center and the middle one an element in between.

Provided the ion beam is still heating the foil after the transition, its center stays very close to the binodal until the rarefaction waves from the foil surface approach the center. The reason for that is the discontinuity in the sound speed on the liquid-vapour coexistence curve. This extraordinary hydrodynamic situation offers a unique possibility to investigate states of matter directly on the binodal. In the calculations presented in [2] an energy deposition of 10 kJ/g for a foil made of  $SiO_2$  is assumed which cannot be realized with ion beam at HHT. For moderate beam intensities high-Z low-melting-temperature targets would be preferable. According to the simulations done with the EOS provided by the FEOS-code [3], an energy deposition of 1 kJ/g would be enough for e.g. a  $Bi$  target to perform an experiment. In first experiments it is essential to verify the assumption of explosive boiling, the nearly instantaneous transition from metastable liquid into the stable liquid-gas mixture. This can be done by detection of the predicted jump in the expansion velocity due to transition to the

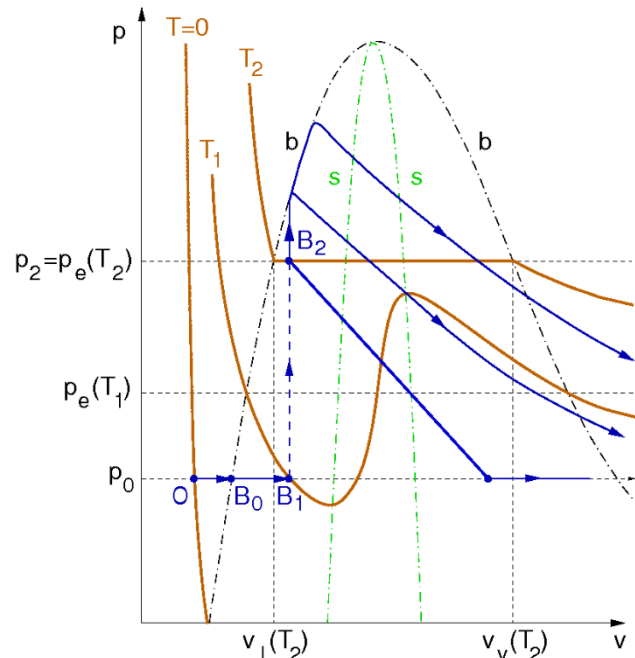


Figure 1: Temporal evolution of the thermodynamic state of ion-beam heated matter (schematic view).

phase equilibrium accompanied by a rapid increase of pressure  $p_0 \rightarrow p_2$  [2].

The material properties of a metastable liquid before the transition can be diagnosed without temporal resolution since all thermodynamic variables in the foil are distributed uniformly in the direction of beam propagation. Furthermore, the knowledge of the beam parameters together with the energy deposition by the ions would immediately provide the internal energy because the kinetic energy for quasi-static isobaric expansion is negligible. Once the transition to equilibrium took place, temporally and spatially resolved measurements are necessary. Since the center of the target remains virtually on the binodal as long as release waves from the target surface don't arrive, the knowledge of only two (and not three) thermodynamic variables is sufficient to obtain a point on the binodal. The calculations show that the beam-target configuration can be optimized to ensure a low fraction of kinetic energy in the target center (below 3 %). Hence, to this accuracy, the energy deposited by the ion beam corresponds to the internal energy on the binodal and it would be sufficient to measure only one thermodynamic variable.

### References

- [1] I. Iosilevskiy, GSI Report GSI-2007-2, May 2007.
- [2] S. Faik, M. Basko, An. Tauschwitz, I. Iosilevskiy, J. Maruhn, High Energy Dens. Phys. 8 (2012) 349.
- [3] S. Faik, An. Tauschwitz, I. Iosilevskiy, Comput. Phys. Commun. 227 (2018) 117.

**Experiment beamline:** SIS18-HHT  
**Experiment collaboration:** APPA-HED@FAIR  
**Experiment proposal:** none  
**Accelerator infrastructure:** SIS 18  
**PSP codes:** none  
**Grants:** BMBF-Projekt 05P15RGFAA  
**Strategic university co-operation with:** Frankfurt



## Prospects of planetary physics research using intense ion beams at FAIR

N.A. Tahir<sup>1</sup>, A. Shutov<sup>2</sup>, I.V. Lomonosov<sup>2</sup>, A.R. Piriz<sup>3</sup>, P. Neumayer<sup>1</sup>, V. Bagnoud<sup>1</sup>, and S.A. Piriz<sup>3</sup>

<sup>1</sup>GSI Darmstadt, Germany; <sup>2</sup>IPCP Chernogolovka, Russia; <sup>3</sup>UCLM Ciudad Real, Spain; <sup>4</sup>HI Jena, Jena, Germany

In this contribution we present a summary of simulation studies that were performed to explore the possibility of employing intense uranium beam to be generated at FAIR to produce planetary core conditions in the laboratory. A dedicated experiment named LAPLAS (Laboratory Planetary Sciences) has been proposed as part of the FAIR High Energy Density (HED) physics program. The beam-target geometry is shown in Figure 1.

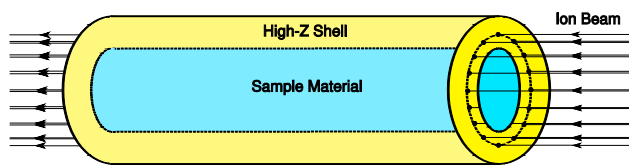


Figure 1: Beam-target geometry of LAPLAS experiment.

The target is comprised of a sample enclosed in a high-Z cylindrical shell. In the present calculations, Fe sample and a W shell have been used. One face of the cylinder is irradiated with a uranium beam with particle energy of 1.5 GeV/u having an annular focal spot that avoids direct heating of the sample by the beam. A 2D hydrodynamic code has been used to study the thermodynamic and the hydrodynamic response of the target. It has been shown that this configuration leads to a multiple shock reflection scheme which generates a low-entropy compression. This means the sample is imploded to ultra-high pressures, super-solid densities but relatively low temperatures. These simulations have shown that using the FAIR uranium beam, one can generate the Earth core conditions as well as those of more massive extrasolar rocky planets, the Super-Earths [1].

These calculations have been thoroughly extended by systematically varying the beam and the target parameters. It has been found that the results are rather insensitive to these changes over a wide parameter range which indicates the stability and robustness of the experimental scheme.

In the present studies the cylinder length is 4 mm while the sample radius is considered to be 0.2 mm and 0.3 mm, respectively. The inner radius of the focal spot ring is assumed to be 0.2 mm, 0.3 mm and 0.4 mm, respectively in the former case. In the latter case, it is considered to be 0.3 mm, 0.4 mm and 0.5 mm, respectively. The width of the focal spot ring is 1 mm.

It is to be noted that an annular focal spot will be generated by using an rf-wobbler that will rotate the beam with high frequency. Since the natural transverse intensity distribution in the focal spot is Gaussian, there always will be some intensity inside the ring that will preheat the sample. To take into account this effect in our studies, we include a linear intensity foot (0, 5, 10, 15 and 20 %) together with parabolic intensity profile in the ring.

Figure 2 shows pressure vs temperature for a particular set of parameters. It is seen that using an intensity of  $2.5 \times 10^{11}$  ions per bunch and a foot level of 5 %, one can generate Earth core conditions with a temperature of 5000 K and a pressure of around 4 Mbar.

Assuming an intensity of  $5 \times 10^{11}$  ions per bunch, one can generate a temperature of about 8000 K and a pressure of 8.5 Mbar, which represent the core conditions of Super-Earth which is few times more massive than the Earth.

It is also seen that considering an intensity of  $10^{12}$  ions per bunch, a temperature of 10000 K and a pressure of 15 Mbar is generated which represents the core conditions of a rocky planet 10 times more massive than the Earth. Further details can be found in [2].

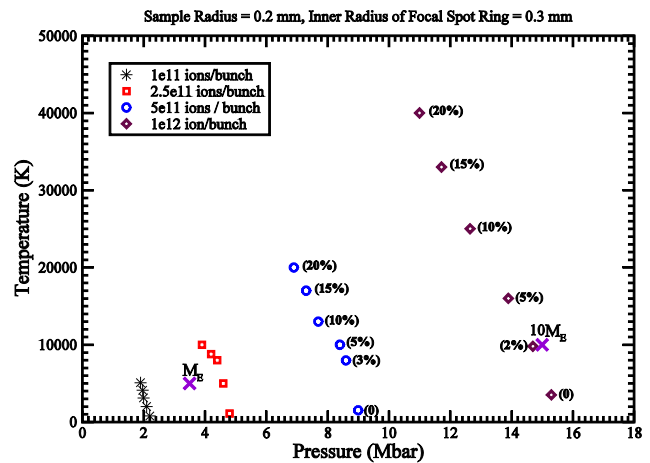


Figure 2: Pressure vs temperature in Fe for different intensities and different foot level, sample radius = 0.2 mm, inner radius of focal spot ring = 0.3 mm and bunch length = 75 ns.

### References

- [1] N.A. Tahir et al., "Studies of core conditions of the Earth and Super-Earths using intense ion beams at FAIR", *Astrophysical J. Supplement Series* 232:1, 2017 September.
- [2] N.A. Tahir et al, Ion beam driven planetary physics research at FAIR, *Astrophysical J. Suppl. Series* (2018) submitted.

**Experiment beamline:** none

**Experiment collaboration:** APPA-HED@FAIR

**Experiment proposal:** LAPLAS

**Accelerator infrastructure:** none

**PSP codes:** none

**Grants:** BMBF

**Strategic university co-operation with:** none

## Investigations on laser-based neutron sources for possible applications\*

M. Zimmer<sup>1</sup>, A. Kleinschmidt<sup>2,3</sup>, S. Aumüller<sup>1</sup>, V. A. Schanz<sup>1</sup>, D. Jahn<sup>1</sup>, J. Hornung<sup>2</sup>, M. Roth<sup>1,4</sup>

<sup>1</sup>Institut für Kernphysik, TU Darmstadt, Germany, <sup>2</sup>Helmholtz-Institut Jena, Germany

<sup>3</sup>GSI Helmholtzzentrum für Schwerionenforschung, Darmstadt, Germany

<sup>4</sup>FAIR –Facility for Antiproton and Ion Research, Darmstadt, Germany

### Introduction

The demand for compact neutron sources is rapidly growing in the last years. To meet this growing need, laser-based neutron sources will play a major role in the upcoming development. These sources can provide neutron beams with maximum energies of several 10s of MeV depending on laser intensity and energy. For many applications, like Neutron Resonance Spectroscopy (NRS) or Neutron Resonance Imaging (NRI), the neutron energy needs to be decreased into the regime of a few eV. This can be done with multiple scattering inside a moderating material. The moderator must be composed of elements that have a low mass for rapid slowing down, while at the same time must have a low neutron absorption cross section. Hydrogen has the lowest mass, but a high absorption cross section, carbon on the other hand has a high mass but a low absorption. Therefore, a moderator out of High Density PolyEthylene (HDPE) is used which consist of C and H atoms in a ratio 1:2.

### Experiment

To test the capabilities of a laser-based neutron source for NRS and NRI, an experiment was designed and conducted at the PHELIX laser as a succession of a beamtime at the Trident laser facility at the Los Alamos National Laboratory, USA[1]. The intended goal was to test a new moderator design and two new neutron detectors.

#### *New moderator design*

Fluka Monte Carlo simulations have shown that a new moderator design could enable a gain of up to 30% more epithermal neutrons into the direction of the detector. This gain is achieved by two modifications to the previous moderator design of earlier experiments [1]. The width of the rear part in the direction of the detector, was decreased by two centimetres to 5 cm as seen in Figure 1. This reduces absorption by hydrogen during moderation and minimizes the neutron Time of Flight (ToF) pulse width which is mainly limited by the time neutrons diffuse inside the moderator before they reach the HDPE surface. The second modification is the addition of two HDPE wings at the front of the moderator. These wings are able to capture and moderate neutrons, that are emitted with an angle between 90° and 146° towards the TNSA axis, which otherwise would have been lost for experimental purposes.

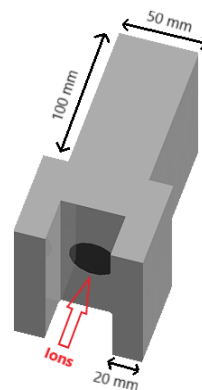


Figure 1: New moderator design with rear part reduced to 50 mm width and including two wings at the front side for moderating additional neutrons.

#### *Testing of new neutron-ToF detector*

The ToF detector is made of two 100x100mm borated Multi Channel Plates (MCP) in chevron configuration and an anode. Boron has a high cross section for (n,α) reactions. The emitted α-particles produce electrons in the MCP which are amplified and can be detected as a current on the anode. With this detector it was possible to distinguish between single neutron absorption events with a 10 ns temporal resolution. For higher neutron fluxes, the current can be seen as proportional to the amount of counted neutrons. Experiments have shown, that a high amount of neutron shielding around the detector is necessary to prevent scattered neutrons from the chamber walls from interfering with the ToF measurement.

#### *NRI detector*

In addition to the NRS detector, a NRI detector consisting of a lithium glass scintillator and a fast gateable camera system was tested. The detector was placed in a distance of 1.1 m from the moderator in 90° towards laser forward direction. Scattered neutrons in this direction were shielded by a collimator made out of borated HDPE. In front of the scintillator several materials with high neutron absorption cross sections and absorption resonances were placed with the intent to distinguish between different samples in the image. As a result of this beamtime, it is possible to say that the detector can distinguish between a blocked and a free neutron flight path but for neutron resonance imaging, the signal to noise ratio has to be advanced and the neutron flux improved. For instance this can be done by using a larger light capturing system, decreasing the distance between scintillator and camera or by cooling the imaging system to reduce the camera noise.

### References

- [1] GSI Scientific Report 2016, DOI: 10.15120/GR-2017-1 RESEARCH-APPA-PP-11 P281

\* This report is also submitted to “High Energy Density Physics Report 2017”

**Experiment beamline:** PHELIX  
**Experiment collaboration:** APPA-PP  
**Experiment proposal:** [P151]  
**Accelerator infrastructure:** other: PHELIX  
**PSP codes:** [none]  
**Grants:** [none]  
**Strategic university co-operation with:** Darmstadt

## Moderation of laser-driven neutrons for Neutron Resonance Spectroscopy

A. Kleinschmidt<sup>1,2</sup>, A. Favalli<sup>3</sup>, A. Tebartz<sup>4</sup>, G.A. Wurden<sup>3</sup>, V.A. Schanz<sup>4</sup>, and M. Roth<sup>4</sup>

<sup>1</sup>GSI, Darmstadt, Germany; <sup>2</sup>HI Jena, Jena, Germany; <sup>3</sup>LANL, Los Alamos, NM, USA; <sup>4</sup>Institut für Kernphysik, TU Darmstadt, Germany

### Introduction

The interaction of neutrons with matter is highly different from that of charged particles or electromagnetic waves. Therefore, they are an interesting research and diagnostic instrument for various applications. One of these is Neutron Resonance Spectroscopy (NRS) which, amongst other things, allows the identification of materials and their elemental composition as well as material-selective imaging of objects. The technique is based on the resonance structure of neutron capture and scattering reactions with matter, which is unique for every element and isotope.

A laser-driven neutron source is based on a high-intensity short-pulse laser irradiating a deuterated polymer foil with a thickness in the range of several 100 nm. The subsequently accelerated ions impinge a beryllium converter (so-called catcher) and generate neutrons via nuclear reactions. The resulting neutron spectrum shows an exponential decay with cutoff energies of a few 10 MeV [1].

However, to apply laser-generated neutrons to NRS, a moderating material has to be used, as a high number of isotopes have pronounced resonances in the epithermal energy range (0.1 eV to 100 keV). The material and geometry of the moderator are designed to maximize the neutron yield in the desired energy range and at the same time minimize the temporal spread of the neutron pulse caused by the additional material.

### Neutron moderation for NRS at Trident

During the experiment at the Trident laser facility at Los Alamos National Laboratory, a polyethylene moderator was used to slow down neutrons emitted by the beryllium catcher. The Trident short-pulse laser had an energy of 80 J and was focused on thin polystyrene foils via a f/1.5 off-axis parabola leading to intensities above  $10^{20}$  W/cm<sup>2</sup> on target.

To maximize the emitted neutron yield, the cylindrical beryllium catcher had a 15×15 mm hole drilled into it facing the incoming ion beam. As can be seen in Figure 1, the catcher was placed inside a high-density polyethylene (HDPE) moderator with a length of 13.8 cm in laser-forward direction and a width of 7 cm in line of sight to the time of flight (ToF) detector, which was set up perpendicular to the laser axis. In addition, a collimator consisting of steel disks and boronated polyethylene blocks was placed in line of sight to the detector to limit the field of view to the neutron source.

The neutrons were detected by a boron- and gadolinium-doped microchannel plate (MCP) with a sensitive area of 28 mm in diameter [2], which was placed inside a metal box and surrounded by thick boronated

polyethylene blocks to shield it from electromagnetic pulses and scattered neutrons. The MCP was set up at a distance of 1.67 m to the neutron source.

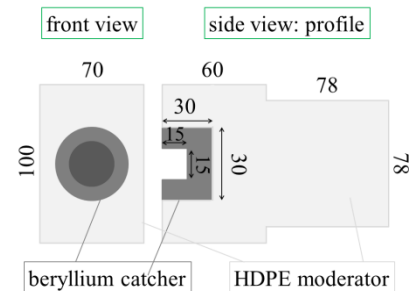


Figure 1: Sketch of the catcher-moderator setup. The accelerated ion beam is impinging the center of the hole. Dimensions are given in mm.

The chosen material for the NRS measurement was indium, which has a pronounced resonance at 1.46 eV. Thus, the neutron yield had to be maximized around this energy. A comparison of neutron energy spectra measured with and without a moderator is shown in Figure 2. The energy range of the plot was chosen around the indium resonance at 1.5 eV. At this specific energy, the moderator causes an increased neutron yield of a factor 3. The difference of both setups is even more pronounced for smaller energies, resulting in an order of magnitude more neutrons at the thermal energy of 25 meV.

These results enable the application of laser-driven neutrons to NRS measurements in the epithermal energy range. During the experiment, the above given indium resonance could successfully be measured [3].

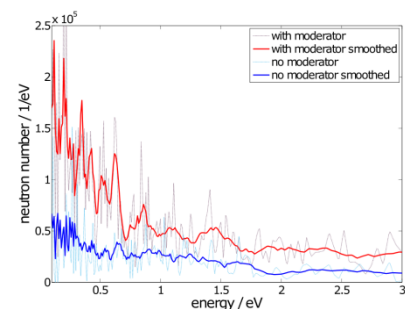


Figure 2: Comparison of neutron spectra obtained from a single laser shot with (red) and without (blue) a moderator around the catcher.

### References

- [1] J.C. Fernández et al., Phys. Plasmas 24, 056702 (2017)
- [2] A.S. Tremsin et al., Nucl. Instrum. Methods Phys. Res. A 539, 287 (2005)
- [3] A. Kleinschmidt, GSI scientific report 2016, p. 281 (2017)

**Experiment beamline:** none

**Experiment collaboration:** none

**Experiment proposal:** none

**Accelerator infrastructure:** none

**PSP codes:** [none]

**Grants:**

**Strategic university co-operation with:** Darmstadt

# Construction, characterization and optimization of a plasma window for FAIR, status update

B. F. Bohlender<sup>1#</sup>, A. Michel<sup>1</sup>, M. Dehmer<sup>1</sup>, M. Iberler<sup>1</sup>, J. Jacoby<sup>1</sup>

<sup>1</sup>IAP, Goethe University, Frankfurt, Germany

## Introduction

The Plasma window is a membrane free beam transition between a region of higher pressure (e.g. Target chamber, gas stripper) and the vacuum of an accelerator. For details on the working principle, the reader is referred to [1], [2], [3].

### Constructional remarks

As described within the last report [1], the thermal stress on all parts of the window, especially the stress on the cathode, proved to be a real challenge. Nearly all parts showed thermal caused damage, the cathode being nearly completely devastated after 15min of operation.

New constructed Cooling plate design and the usage of WIG-welding needles as cathode tips allow to increase the lifetime of the window to at least 5h.

## Experimental results

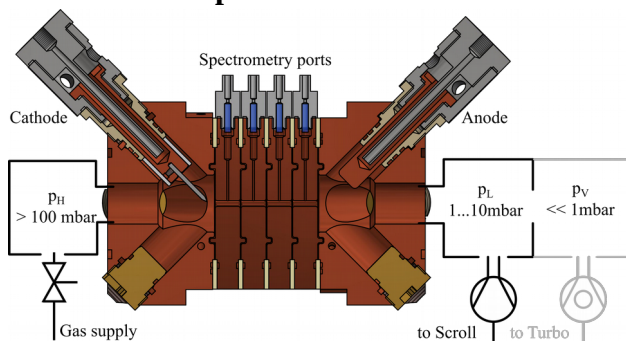


Figure 1: Schematic Setup of pumping stage, the gray turbo-stage has not yet been set up but is due this year.

The data presented herein has been collected with a residual gas composed of Ar with 2% H<sub>2</sub>. Currents between 40A and 60A have been used, while the pressure on the high pressure side ranges from 280mbar to 450mbar, on the low pressure side from 4mbar to 7mbar. The aperture of the discharge channel is 3.3mm.

Figure 1 shows a schematic view of the setup including a cross-section of the current window. High pressure side is to the left, as is the cathode.

### Plasma parameters

First tests of a radial spectrometry setup along the discharge axis enabled the simultaneous determination of (radial integrated) plasma parameters. In comparison to last years data, the electron temperature increased significantly from around 0.5eV to 1.2eV, this is mainly due to the improved cathode construction where now less energy is being deposited into the melting of the material.

## References

[1] B. Bohlender et al GSI HED report 2017

# bohlender@iap.uni-frankfurt.de

In addition, first measurements of the electron density were carried out, showing a strong dependence on the current, pressure and the position inside the discharge channel. Values of  $n_e$  vary from  $0.2 \cdot 10^{16} \text{cm}^{-3}$  up to  $4 \cdot 10^{16} \text{cm}^{-3}$ .

### Pressure parameters

The pressure measurements were carried out while holding the pressure on the low pressure side (i.e. pumping side) constant, thus keeping a constant volume flow through the experiment.

The measurements show that the pressure quotient, that is the pressure on the high side divided by the pressure on the low side, is clearly dependent on the discharge current, and seems to depend on the volume flow. This quotient ranges from almost 60 to over 70, see Fig. 2.

Compared to the quotient measured when no plasma is burning, it's plain to see that the plasma increases the

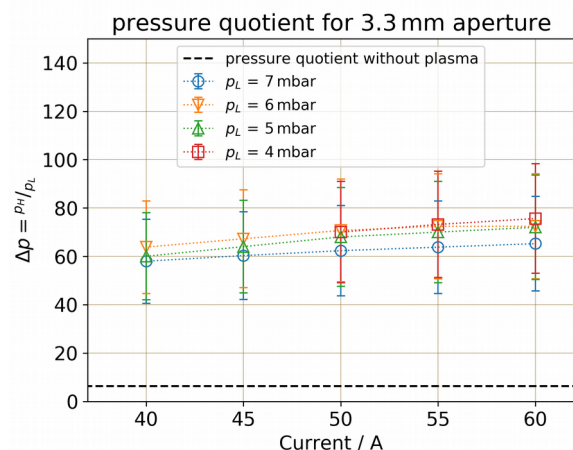


Figure 2: Pressure quotient for different  $p_L$  and currents. Quotient without plasma is around 6-7

quotient by a factor around 10, resulting in the same possible reduction in length over a differential pumping system.

## Conclusion and outlook

The plasma window is operational for well over 5h now and realizing an improvement in the pressure quotient by a factor of 10 when compared to a differential pumping system.

In the near future, the complete differential pumping system, including the turbo-stage, will be build and tested. Additional tests with a larger aperture will be performed.

[2] B. Bohlender et al GSI HED report 2016

[3] A. Hershcovitch, J. Appl. Phys, 1995

**Experiment beamline:** none

**Experiment collaboration:** Hadronenlinacs

**Experiment proposal:** Neu- und Weiterentwicklungen von Beschleunigeranlagen, Detektorsystemen, Verfahren der Physikanalyse

**Accelerator infrastructure:** UNILAC / SIS18

**PSP codes:** none

**Grants:** BMBF: 05P15 RFRBA

**Strategic university co-operation with:** Darmstadt

## Study on a dense and high ionized plasma for ion beam stripping\*

P. Christ<sup>1</sup>, K. Cistakov<sup>1</sup>, T. Ackermann<sup>1</sup>, A. Blazevic<sup>2</sup>, A. Fedjuschenko<sup>1</sup>, R. Gavrilin<sup>3</sup>, M. Iberler<sup>1</sup>, T. Manegold<sup>1</sup>, L. Manganelli<sup>1</sup>, O. Rosmej<sup>2</sup>, S. Savin<sup>3</sup>, K. Weyrich<sup>2</sup>, G. Xu<sup>1</sup> and J. Jacoby<sup>1</sup>

<sup>1</sup>Goethe University, Frankfurt, Germany; <sup>2</sup>GSI, Darmstadt, Germany; <sup>3</sup>ITEP, Moscow, Russia

After a positive "proof of concept" with the screw-pinch and the spherical theta-pinch at a beam time at GSI in 2014 [1,2], a revised version of the theta-pinch has been developed and built for future research [3].

First spectroscopic diagnostics on this revised design have shown a time-averaged peak electron density of about  $1.8 \cdot 10^{16} \text{ cm}^{-3}$  at 60 Pa and 20 kV (see fig. 1), from which a maximum momentary electron density of  $1 \cdot 10^{17} \text{ cm}^{-3}$  is inferable. To gain an even higher electron density, the charging voltage will be increased up to 35 kV. According to a linear behaviour of the maximum electron density and the discharge energy [4], a maximum momentary electron density of approximately  $5 \cdot 10^{17} \text{ cm}^{-3}$  and an advance of the electron temperature from 1 eV up to 4 eV is expected from the increased discharge energy.

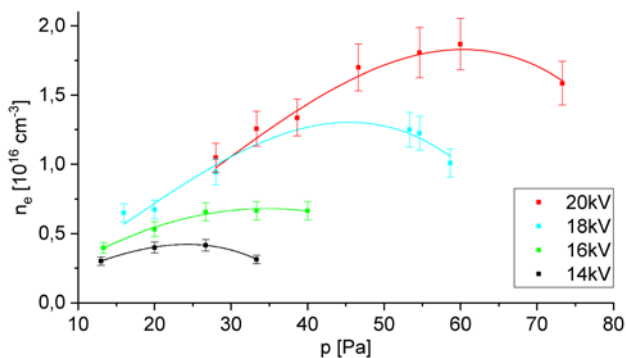


Figure 1: Time-averaged electron density at different pressures and load voltages.

Additionally, the spiral cylindrical shape of the new coil offers two basic advantages. On one hand, the ion beam transmission through the plasma cell is enhanced due to a more symmetrical magnetic field and on the other hand, the axial plasma exhalation displaces undesired residual gas between the vessel and the differential pumping system, extending the plasma ion beam interaction zone. The new design has been tested for its serviceability at GSI in 2016 and will be applied at a beam time at GSI in 2018. Besides researchers from Goethe University, Frankfurt, this beam time will be conducted by scientists from other facilities such as ITEP, Moscow, IMP, Lanzhou and IUAC, New Delhi, who are studying on the same topic.

For a better understanding of the internal plasma processes, multiple time-resolved spectroscopic diagnostics as well as a laser interferometry are intended. The interferometric diagnostic will be based on previous investigations, which have focused on finding a suitable basic scheme and pre-setting main operation parameters such as wavelength and time resolution [5]. Since a high electron density of the order  $10^{17} \text{ cm}^{-3}$  is expected, to restrict the all

\* This report is also submitted to the report "News and Report from High Energy Density generated by Ion and Laser beams 2017".

over phase shift to lower the standards for the scope, to have a simpler alignment and to limit the influence of a potentially existing density gradient, short wavelengths in the visible range are favoured.

During interferometric test measurements on a small-scale z-pinch, a suspected disturbing influence of electromagnetic noise has occurred. Consequently, a sufficient metallic shielding of the interferometer and its vulnerable electric components in a separate set-up as well as an improvement of the signal-to-noise ratio by a raised laser power are designated. To transfer the laser beam towards and back from the plasma experiment, a fibre connection will be investigated.

Figure 2 shows a first draft of the interferometer for future time-resolved measurements of the electron density.

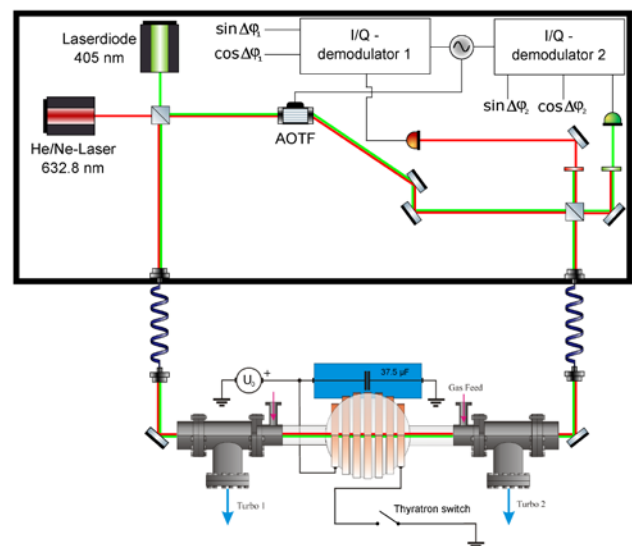


Figure 2: First draft of the future interferometer set-up.

A novel combination of an acousto-optic heterodyne technique and a two-colour vibration compensation with wide separated wavelengths is illustrated. If the vibrational contribution is negligible to the plasma contribution, the second wavelength could be utilized to estimate the ionization degree, which would lead to a precise measurement of the electron temperature. In addition, an acousto-optic tuneable filter (AOTF) will be tested as a solution for maintaining the required collinearity of the wavelengths.

## References

- [1] G. Xu *et al.*, Phys. Rev. Lett. **119**, 204801 (2017).
- [2] G. Xu *et al.*, GSI SCIENTIFIC REPORT 2014, AP-PA-MML-PP-16.
- [3] K. Cistakov *et al.*, GSI SCIENTIFIC REPORT 2016, RESEARCH-APPA-PP-22.



- [4] C. Teske *et al.*, *Physics of Plasmas* **19**, 033505 (2012). [5] P. Christ, Master thesis, 2017

**Experiment beamline:** Z6

**Experiment collaboration:** APPA-HED@FAIR, Research group "Hadron Accelerators"

**Experiment proposal:** U275, U306, U317

**Accelerator infrastructure:** UNILAC

**PSP codes:** none

**Grants:** BMBF No.: 05P15RGFAA and 05P15RFRBA, HGS-HIRe

**Strategic university co-operation with:** Darmstadt

## Cone compression of a pulsed plasma sheath

T. Manegold<sup>1</sup>, S. Faik<sup>1</sup>, C. Benzing<sup>1</sup>, P. Tavana<sup>1</sup>, J. Wiechula<sup>1</sup>, M. Iberler<sup>1</sup> and J. Jacoby<sup>1</sup>

<sup>1</sup>Goethe University of Frankfurt, Frankfurt am Main, Germany.

### Introduction

Coaxial plasma accelerators (CPA's) have been investigated in different experimental configurations in the past, with applications to space propulsion [1], plasma refueling for fusion reactors [2] and as a high voltage switch [3]. The purpose of the presented project is the application as an intense UV/VUV back lighter source. The wavelength spectrum of the emitted light depends on the excited states, whereas the intensity is in correlation to the electron density. The plasma sheath of the utilized CPA has been characterized in [4]. To increase electron density and to extend the emitted spectrum to lower wavelengths, the plasma is compressed by a glass cone after acceleration phase.

### Experiment and Results

The experiment is driven by a CPA, whose pulse forming network has a total capacitance of 27 $\mu$ F with a maximum voltage of 10kV. Due to the high current of up to 150 kA, the Lorentz force accelerates the plasma to velocities in the 10 km/s range.

The electron density determination of the uncompressed plasma has been performed time and spatially integrated by the common method of linear Stark-broadening of the H $\beta$  line. This method is however only applicable at the beginning of the compression. Then, due to the high electron densities, this line is broadened too widely to be utilized. As an alternative, the broadening according to the quadratic Stark-effect of a copper line at 479.40nm was applied. It was possible to cross calibrate this line with the H $\beta$  line at lower densities. Doing so, we obtain

$$n_e [\text{cm}^{-3}] = C \cdot \Delta \lambda_s [\text{nm}] \quad (1)$$

with the calibration factor of  $C=(3.07\pm 0.475) \cdot 10^{18}$ .

In a first cone, which is characterized by an opening at the end of 5mm and a tapering angle of 26.5 $^\circ$ , the electron density could be increased from initially several  $10^{15}\text{cm}^{-3}$  in

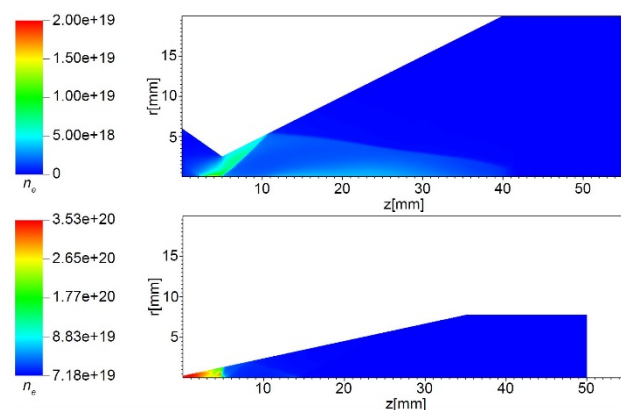


Figure 1: Simulation of the electron densities in different cone shapes at the time of maximum value with first cone (top) and optimized cone (bottom).

the uncompressed plasma cloud to about  $10^{18}\text{cm}^{-3}$  at the tip of the cone at a charging voltage of 9kV and a Helium gas pressure of 15mbar. Two-dimensional hydrodynamic simulations of the compression have been performed with the RALEF-2D code. According to these simulations (Fig. 1), the electron density can even be increased by changing the cone parameters to a tiny opening of 0.5mm and a tapering angle of 12 $^\circ$ . The discrepancy of the density values between simulation and experiment is assumed to be unobserved by the highly time dependant changes and additional radiation losses, not taken into account in the code.

The experimental results of the electron density at  $U=5\text{kV}$  and  $p=5\text{mbar}$  are depicted in Fig. 2 in dependence of the position  $z$ . As can be seen, although voltage and gas pressure are reduced, an optimized cone compressed the plasma to electron densities comparable to the values of the first cone at 9kV and 15mbar. Compared to the uncompressed values, the compression increases the electron density by about a factor of 630.

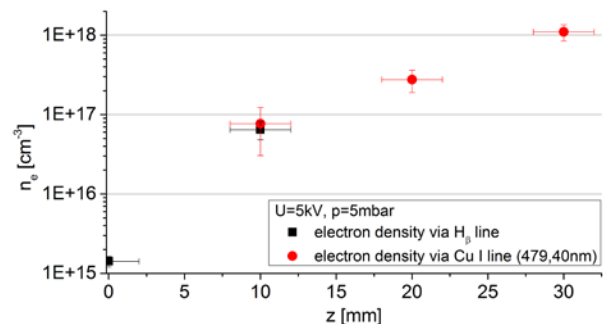


Figure 2: Electron densities in the optimized cone

Additionally, the observed emitted wavelength has expanded at higher densities from wavelengths above 97.25nm to a wavelength range starting already at approximately 53.70nm. Our next step is to replace the fragile glass by a different material to be able to perform the compression at higher voltages and pressures to increase electron density even more. According to the RALEF-2D simulations, this could increase the compressed density by a further order of magnitude.

### References

- [1] D. Y. Cheng, "Application of a deflagration plasma gun as a space propulsion thruster," *AIAA Journal*, vol. 9, no. 9, pp. 1681–1685, Sep. 1971.
- [2] D. Witherspoon, et al., "A contoured gap coaxial plasma gun with injected plasma armature," *Review of Scientific Instruments*, vol. 80, no. 8, 2009

- [3] M. Iberler, et al., “Optical and electrical investigations of a high power Lorentz drift based gas discharge switch,” IEEE ICOPS, June 2008, pp. 1–1.
- [4] T. Manegold, et al., “Generation and characterization of a pulsed dense plasma with helium,” IPMHVC, pp. 580–584, July 2016.

**Experiment beamline:** none

**Experiment collaboration:** APPA-HED@FAIR

**Experiment proposal:** none

**Accelerator infrastructure:** none

**PSP codes:** none

**Grants:** none

**Strategic university co-operation with:** Frankfurt-M

## Acceleration of plasma-propelled flyer plates\*

*S. Sander<sup>1</sup>, J. H. Hanten<sup>1</sup>, M. M. Basko<sup>2</sup>, An. Tauschwitz<sup>3</sup>, G. Schaumann<sup>1</sup>, D. Schumacher<sup>4</sup>,  
A. Blazevic<sup>4</sup> and M. Roth<sup>1</sup>*

<sup>1</sup>Technische Universität Darmstadt, Institut für Kernphysik, Darmstadt, Germany; <sup>2</sup>Keldysh Institute of Applied Mathematics RAS, Moscow, Russia; <sup>3</sup>Goethe Universität, Frankfurt, Germany; <sup>4</sup>GSI Helmholtzzentrum für Schwerionenforschung GmbH, Darmstadt, Germany

\* This report is also submitted to "News and Reports from High Energy Density generated by Heavy Ion and Las

### Introduction

Man-made space debris is exponentially increasing in the low earth orbit, posing a big threat on current and future space missions [1]. To remove this space debris, high velocity impacts ( $v > 10$  km/s) of tungsten balls with a presumed momentum transfer factor of  $\sim 10$ -15 are proposed to slow down space debris [2]. Thereby, it will decrease in orbit and burn up in the atmosphere sooner.

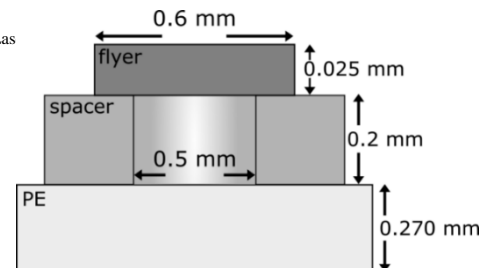
### Experiment

For preliminary experiments in this area of high velocity impacts, a special target design has been developed as seen in figure 1. The objective is the acceleration of a high velocity, solid state tungsten flyer plate for future impact experiments.

Previous experiments, using different target designs, failed to show an acceleration of the flyer but suggested an evaporation of the tungsten disk. Therefore, a target design which allows for a completely free flyer is developed. The target consists of three layers. The bottom layer is a 270  $\mu\text{m}$  thick polyethylene (PE) sample. A steel spacer of 200  $\mu\text{m}$  thickness and with a 500  $\mu\text{m}$  diameter hole is glued on top of the PE. The hole is covered with a tungsten disk with a diameter of 600  $\mu\text{m}$  and 25  $\mu\text{m}$  thickness. In this setup, the to be accelerated disk is completely free and not glued to any structure.

The experiments are performed at the target area Z6 at GSI, where the nhelix laser system is used to drive a shock wave into the PE. After the shock breakout, the material expands through the hole and hits the disk. This is supposed to accelerate the tungsten to high velocities, while retaining its solid state. As the target is driven from below, a completely new beam path is put in place. The beam is guided through the bottom flange and focused with a lens and random phase plate onto the PE. A laser energy of 2 J is used to ensure the integrity of the accelerated disk.

The targets rear side is observed with two DICAM Pro in a side view configuration with a relative angle of 90° between them. In figure 2, the recorded images can be seen. A background is subtracted to enhance the visibility of the disk for one of the cameras (figure 2a). The disk is observed in flight in both images. The disk clearly rotates, which is thought to originate from a non-uniform plasma expansion inside of the steel spacer. From the two different images and the time delay a velocity of about  $110 \pm 4$  m/s is deduced. With a streak camera the disk movement is observed over a time window of 1000 ns around the expected time of acceleration. The movement



speed was determined through linear approximation to  $100 \pm 30$  m/s.

Figure 1: Schematic of the layered target design. A steel spacer is glued on top of a polyethylene foil (PE). The flyer is made of tungsten and placed without fixation. The target is driven from below, accelerating the plasma and flyer upwards.

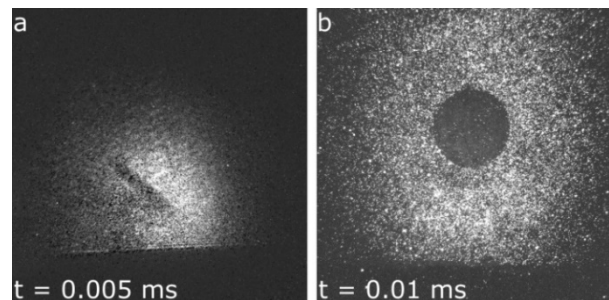


Figure 2: Recorded images of the two DICAM Pro. A background image is subtracted from image (a) to increase visibility. The flyer is clearly seen in both images, rotating rather than flying straight up.

### Simulation

Simultaneously, hydrodynamic fluid simulations in two dimensions are performed with the RALEF code [3,4], to further study the target. These simulations with a laser energy of 2 J are in good agreement with the measured velocities, calculating the flyer velocity to 101 m/s. In addition, the simulations suggest a fluid pressure of 19 kbar inside the tungsten. This value closely corresponds to the tensile strength of tungsten, explaining previous failures of the targets driven with higher intensities.

### References

- [1] D. McKnight, D. Kessler, IEEE Spectrum, Retrieved (2012).
- [2] G. Ganguli et al., Aerospace Conference, 2012 IEEE (2012).
- [3] M. M. Basko, J. Maruhn, A. Tauschwitz, J. Comp. Physics, 228, (2009)
- [4] M. M. Basko, J. Maruhn, A. Tauschwitz, GSI-Report 2010-1, PLASMA-PHYSICS-25 (2010)

**Experiment beamline:** Z6  
**Experiment collaboration:** none  
**Experiment proposal:** none  
**Accelerator infrastructure:** none  
**PSP code:** none  
**Grants:** none  
**Strategic university co-operation with:** Darmstadt

